STUDIES TOWARDS THE TOTAL SYNTHESIS OF THE MACROCYCLIC DIAMINE ALKALOID HALICLONACYCLAMINE C

A Thesis

by

TAO QU

Submitted to the Office of Graduate Studies of
Texas A&M University
in partial fulfillment of the requirements for the degree of

MASTER OF SCIENCE

August 2004

Major Subject: Chemistry

STUDIES TOWARDS THE TOTAL SYNTHESIS OF THE MACROCYCLIC DIAMINE ALKALOID HALICLONACYCLAMINE C

A Thesis

by

TAO QU

Submitted to the Office of Graduate Studies of
Texas A&M University
in partial fulfillment of the requirements for the degree of

MASTER OF SCIENCE

Approved as to style and content by:

Gary Sulikowski (Chair of Committee)	Howard Williams (Member)
Daniel Singleton (Member)	Emile Schweikert (Head of Department)
Daniel Romo (Member)	

August 2004

Major Subject: Chemistry

ABSTRACT

Studies towards the Total Synthesis of the Macrocyclic

Diamine Alkaloid Haliclonacyclamine C.

(August 2004)

Tao Qu, B.S., Peking University

Chair of Advisory Committee: Dr. Gary A. Sulikowski

Marine sponges produce a series of complex polycyclic diamine alkaloids which appear to have a common biogenesis from simple bis-pyridine macrocycles. These structurally novel secondary metabolites are presumably biosynthetically produced by the controlled ionic coupling of macrocyclic 3-alkyl piperidines leading to 3,4'-linked bis-piperidines (**ii**). Included among these diamine marine alkaloids is haliclonacyclamine C (**i**) which serves as our synthetic target.

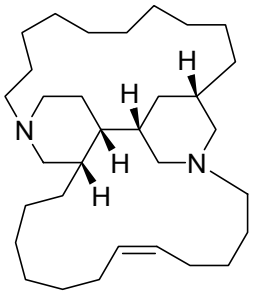

haliconacyclamine C (**i**)

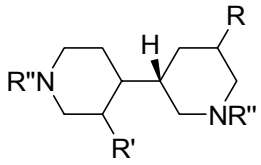

3,4'-linked bis-piperidines (**ii**)

Chapter I in this thesis provides background information describing biological activity and proposed biosynthetic pathways to these important diamine marine alkaloids. Chapter II details progress towards the total synthesis of haliclonacyclamine C. The focus of Chapter II will be on our successful construction of the 3,4'-linked bispiperidine central core (**ii**) highlighted by the use of palladium-mediated C-C bond forming processes. The stereoselective hydrogenation of a coupled product will also be discussed.

To my dear mom, dad and my lovely wife!

ACKNOWLEDGEMENTS

I would like to deeply thank my capable, caring and awesome advisor, Professor Gary A. Sulikowski, for his guidance and support during my graduate study at Texas A&M University. My appreciation is extended to those faculty members who have invested their time by serving on my committees during my career at Texas A&M University: Dr. Singleton, Dr. Daniel Romo and Dr. Williams. I also want to thank the Laboratory for Molecular Simulation for providing me training and assistance in applying molecular modeling in my research. In addition, I am indebted to Dr. Burgess, Dr. Pennington and Dr. Michelle Sulikowski for their kind help in my application for future Ph.D. study.

I have thoroughly enjoyed my time spent with the members of the Sulikowski group both past and present as well as my friends in other research groups. I would like to thank Bin Wu, who served as my mentor when I first joined the group and provided me excellent instruction in laboratory technique and chemistry knowledge. A special thank you goes to Dr. Weidong Liu for his inspiration, friendship and sharing his point of view of life with me. In addition, my appreciation goes to Dr. Umar S. M. Maharoof, Dr. Ron Pongdee, Dr. Kwangho Kim, Dr. Steve Luo, Dr. Bohan Jin, Dr. Kurt Kiewel, Brant Boren and Qingsong Liu for stimulating chemistry discussions as well as their friendship over the years.

I could not have survived this journey without the loving and caring support of my family. In particular, my heartfelt appreciation goes to my wonderful wife Sha, for

enduring the hardship of our not being together over the past two years since we got married. What I can say is that you are the best thing that has ever happened to me and that my life would be meaningless without you. To my dearest Mom and Dad, thank you for your never-ending love, encouragement and support over the past twenty-five years. I apologize for not being with you for so long.

TABLE OF CONTENTS

CHAPTER Page

LIST OF FIGURES

FIGURE Page

LIST OF SCHEMES

SCHEME Page

LIST OF TABLES

CHAPTER I

INTRODUCTION TO MARINE MACROCYCLIC DIAMINE ALKALOIDS: SIGNIFICANCE AND BIOSYNTHETIC PATHWAYS

1.1 Background and Biological Importance of Marine Secondary Metabolites

Secondary metabolites are compounds produced by organisms which are presumably not directly needed for their normal functions. There exist many theories why organisms produce secondary metabolites. One popular belief is that "they are used to store excess nitrogen for later use".[1] This theory seems to have largely arisen because many secondary metabolites contain nitrogen. Another widely held belief is that "they are involved in defense of the organism against threatening organisms and animals".[1] Some scientists subscribe to neither of these beliefs since many secondary metabolites neither contain nitrogen nor do they appear to protect the organism from any predators. In contrast to the initial beliefs that the secondary metabolites do not play a significant role in the life of an organism, many now believe that, either by lucky coincidence or evolutionary necessity, secondary metabolites play a vital role in the life of the producing organism. In addition many secondary metabolites are important in communication between individuals of a particular species. As for the term alkaloid, it is rather a broad term which describes natural products which have a basic nitrogen atom. This is one of the largest groups of secondary metabolites and contain an amazing diversity of structure and biological activity.[1]

This thesis follows the style of the *Journal of Organic Chemistry*.

The study of secondary metabolites has played a major part in the development of organic and medicinal chemistry. Marine organisms produce a fascinating array of structurally novel secondary metabolites, many of which possess potentially significant biological activity. A growing collection of complex and structurally diverse marine macrocyclic alkaloids have been isolated from marine sponges in the last two decades, that are related to each other by a common biogenetic pathway starting from macrocycles composed of 3-alkylpyridine or reduced 3-alkylpyridine units[2-4] (Figure 1).

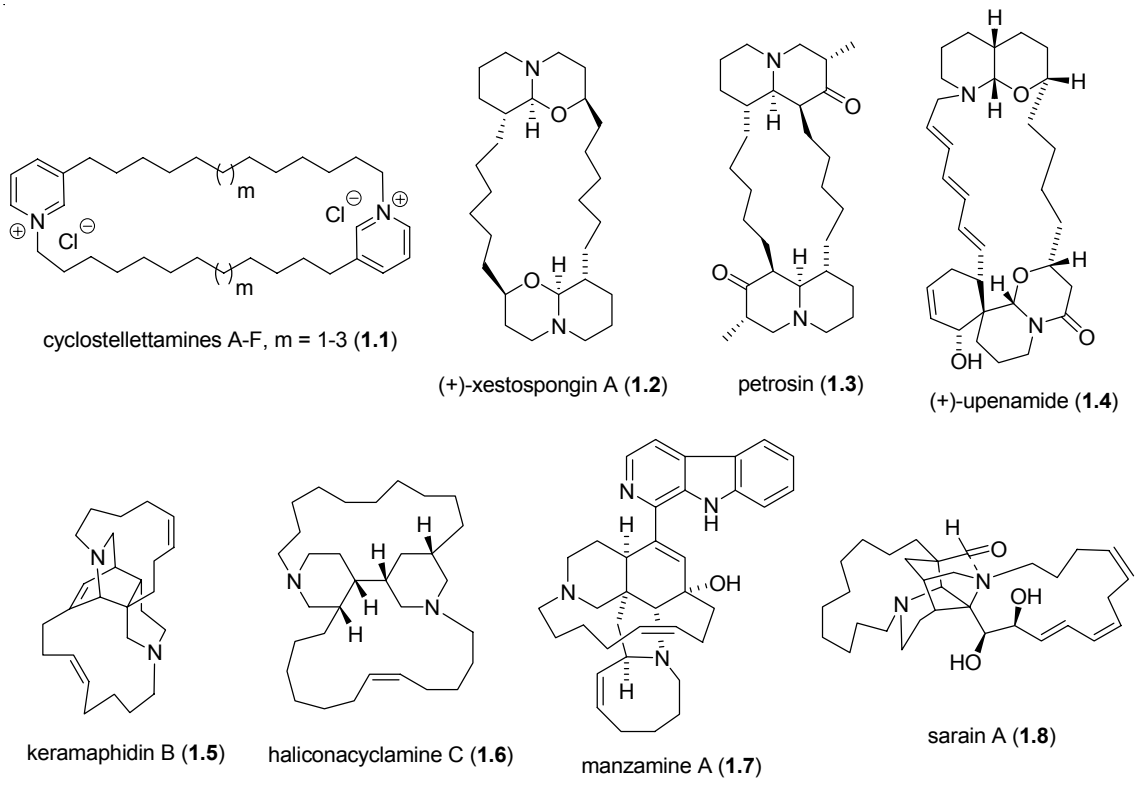

Figure 1 Structures of some marine secondary metabolites isolated from marine sponges

The first member of this exclusively sponge-derived alkaloid family was reported by Higa[5] in 1986 and by Nakamura[6] in 1987. The same compound (**1.7**) was described by both groups, but was given different names: manzamine A (**1.7**), isolated from a *Haliclona* sp. and keramamine A, obtained from *Pellina* sp., respectively. Among related marine alkloids identified, in order of increasing structural complexity, are cyclostellettamine (**1.1**), xestopongin (**1.2**), petrosin (**1.3**), upenamide (**1.4**), keramaphidin B (**1.5**), haliclonacyclamine C (**1.6**), manzamine A (**1.7**) and sarain A (**1.8**) (Figure 1).

1.2 Baldwin's Proposed Biosynthetic Pathway to Manzamine Alkaloids

The isolation of manzamine A (**1.7**), a marine alkaloid possessing a distinctly unique and unprecedented structure, elicited the following statement from Higa, "its [manzamine A's] provenance is problematical as there appears to be no obvious biogenetic path."[5] This challenging problem was clearly taken as an irresistible challenge by Baldwin and coworkers who, in response, published a nonexperimental paper outlining a biosynthetic pathway leading to the entire family of manzamine alkaloids.[7] Their biosynthetic pathway not only revealed the structural symmetry hidden within the complex architecture of the manzamine alkaloids, but also provided a biosynthetic basis that ties the manzamines to an amazing array of structurally diverse and seemingly unrelated marine natural products. Thus, the unique and seemingly unrelated secondary metabolites shown in Figure 1, as we shall see, are proposed to share a common biogenetic origin.

The following discussion describes Baldwin and co-workers' biosynthetic proposal for the manzamine alkaloids. Subsequent experimental evidences support their hypothesis as well.

1.2.1 Details of Baldwin's Biosynthetic Proposal

The group of manzamine alkaloids contains three structural types, represented by manzamine A (**1.7**)[5], B (**1.9**) and C (**1.10**)[8-9] (Figure 2).

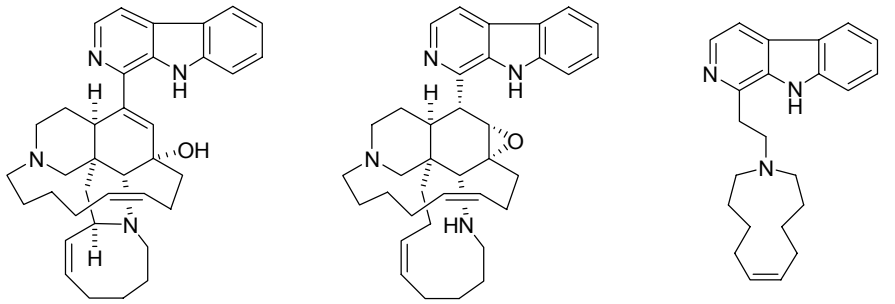

Figure 2 Structures of manzamines A-C

Manzamine C (**1.10**), the least complicated alkaloid of this group, can be reduced to four simple units, tryptophan (**1.11**), a C3 unit (acrolein) (**1.12**), a C10 unit (a symmetrical dialdehyde) (**1.13**) and ammonia (Scheme 1). Condensation of these units would in principle give manzamine C (**1.10**).

Scheme 1 Biogenetic origin of manzamine C proposed by Baldwin

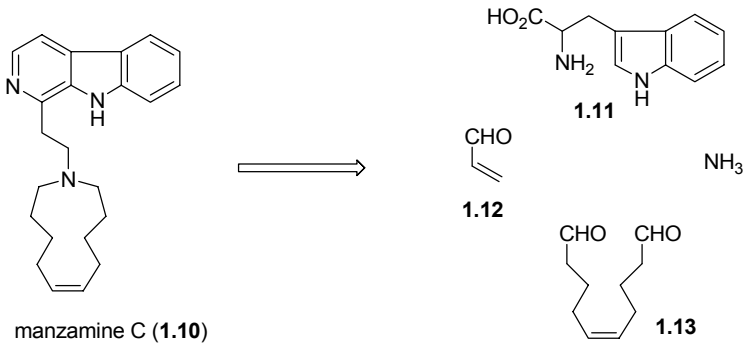

The biosynthesis of manzamine B (**1.10**) is likely to start with protonation of bis-dihydropyridine (**1.14**), derived from two acrolein units (**1.12**), two symmetrical dialdehyde units (**1.13**) and two ammonia units (Scheme 2). Intramolecular Diels-Alder cycloaddition of **1.15** leads to an advanced intermediate **1.16** with the correct relative stereochemistry and connectivity following from the expected endo and regiochemical preference of this cycloaddition. Redox exchange of **1.16** gives immonium species **1.17**, which is hydrolyzed to an aldehyde **1.18**. Finally, condensation of tryptophan (**1.11**) and **1.18** furnishes manzamine B (**1.9**).

Scheme 2 Biogenic origin of manzamine B proposed by Baldwin

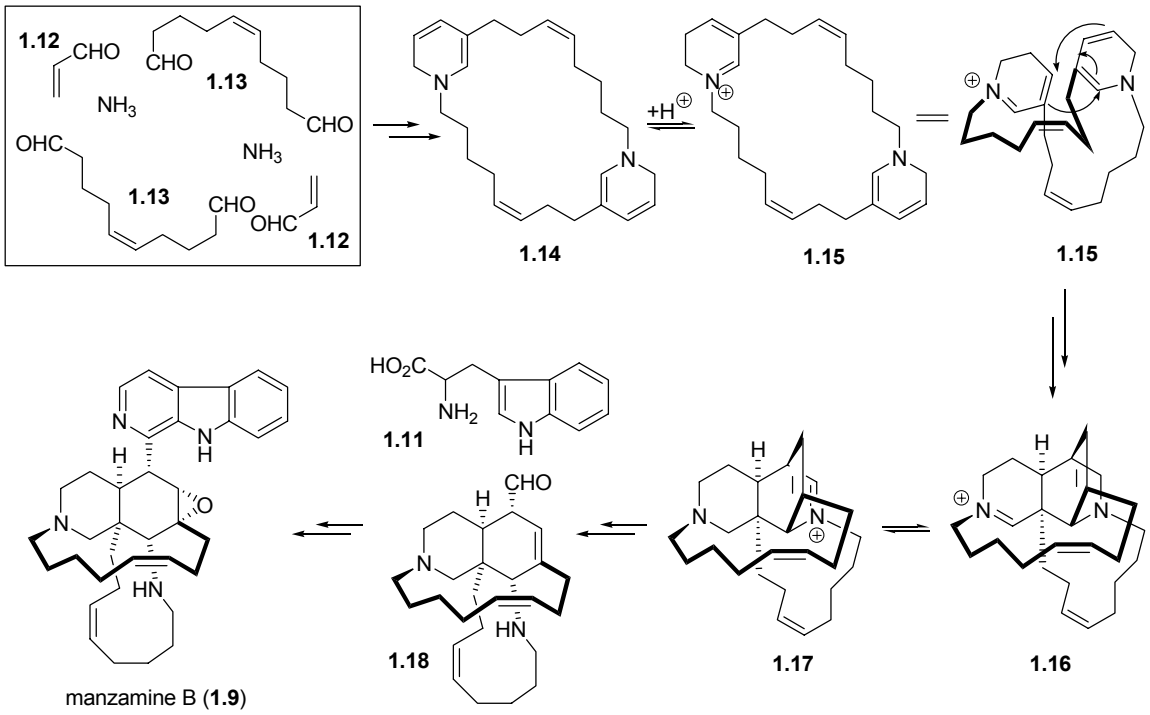

Having described the biosynthesis of manzamine B, only three steps are required to convert manzamine B to manzamine A (**1.7**) (Scheme 3). First, epoxide rearrangement of **1.9** generates intermediate **1.19**. Then carbon-carbon double bond isomerization followed by allylic oxidation gives intermediate **1.20**, which is cyclized to provide the manzamine A (**1.7**). Notably, saturated macrocyclic bis-piperidine intermediates related to **1.15** had earlier been proposed by Cimino and co-workers to serve as biosynthetic precursors to xestopongin (**1.2**), petrosin (**1.3**) and sarain (**1.8**) alkaloids (Figure 1).[10]

Scheme 3 Biogenetic origin of manzamine A proposed by Baldwin

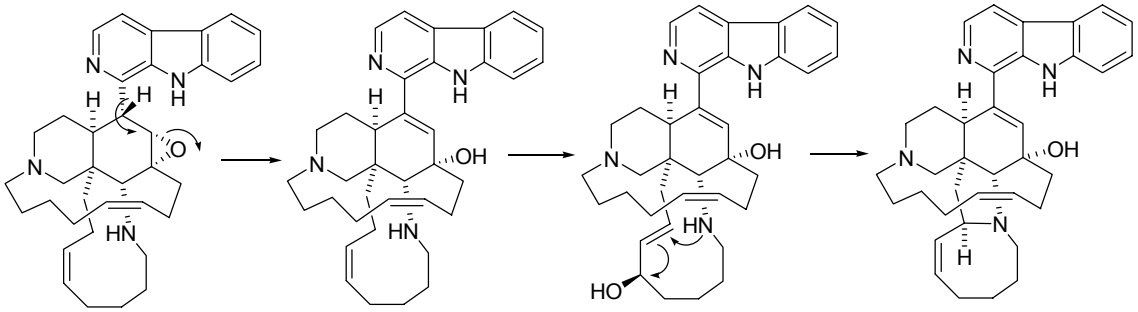

1.2.2 Other Marine Natural Products Isolated Supporting Baldwin's Biosynthetic Proposal

Since the publication of Baldwin's hypothesis, a growing number of manzamine alkaloids have been isolated from various species of sponge worldwide supporting the biosynthetic pathways to the marine sponge secondary metabolites summarized in Scheme 2. For example, the cyclostellettamines A-F (**1.1**) isolated from the marine sponge *stelletta* sp. in 1994 represent oxidized versions of the proposed intermediate **1.15** (Figure 3) presented in Baldwin's proposal described in Scheme 2. Another example is keramaphidin B (**1.5**), which was independently isolated by both the Kobayashi and Anderson groups.[11,12] Structurally keramaphidin B (**1.5**) is the reduced form of the proposed cycloadduct (**1.16**) shown in the Baldwin's manzamine biosynthetic hypothesis. Other isolated natural products include ircinal B (**1.21**), which resembles the proposed intermediate **1.18**.

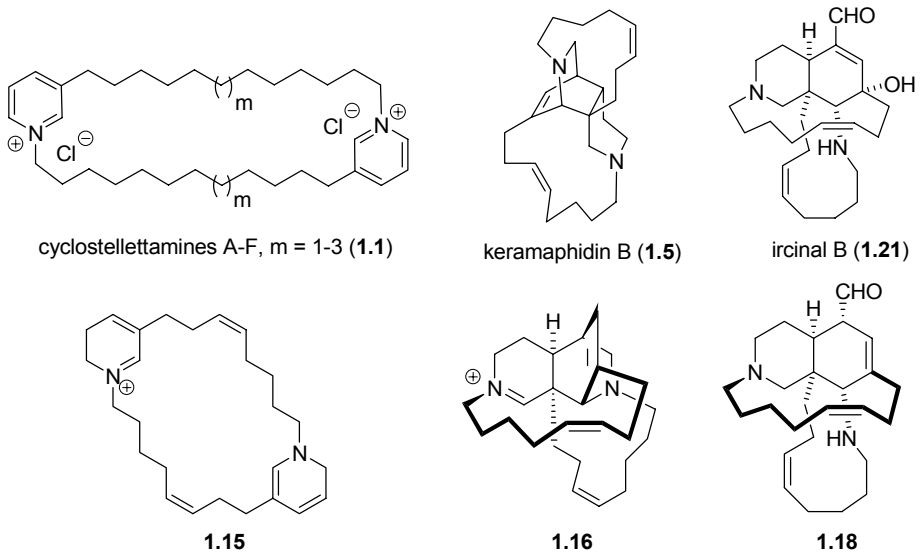

Figure 3 Similarity between natural products and intermediates in Baldwin's proposal

1.2.3 Experimental Evidence Supporting Baldwin's Proposal

To date, no *in vivo* (i.e. labeling studies) have been described to support the proposed biosynthetic pathways outlined in Scheme 2. However, in 1998 Baldwin and Whitehead pursued a biomimetic approach to the manzamine alkaloids focusing on the presumed Diels-Alder cycloaddition step (Scheme 4).[13,14] The synthesis of **1.24** was accomplished via a five-step reaction sequence starting from hydroxyphosphonium salt **1.22** and 3-(3-pyridyl)propanal **1.23**. Oxidation of **1.24** with *m*-CPBA furnished a mixture of N-oxides, which were treated with trifluoroacetic anhydride to give bis-dihydropyridine **1.25**. It was eventually discovered that dissolution of **1.25** in an aqueous methanol buffer, followed by reduction, yielded a very small but detectable amount of cycloadduct keramaphidin B (**1.5**) within a complex mixture of products. Although the yield of the key reaction Diels-Alder cycloaddition was very low (0.2 – 0.3% yield),

Baldwin and co-workers have demonstrated the chemical feasibility of their theoretical proposal for the biogenetic origin of the manzamine alkaloids.

Scheme 4 Baldwin's biomimetic approach to keramaphidin B

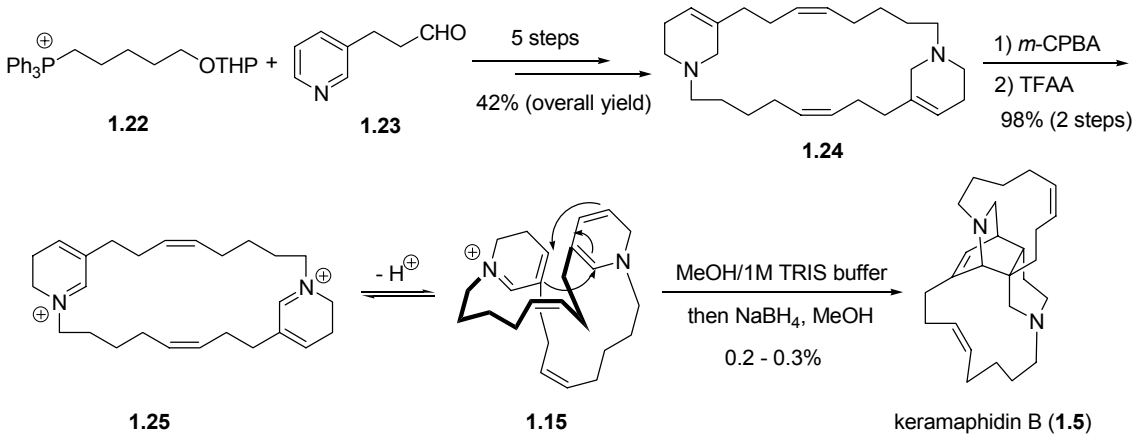

1.3 Biosynthetic Pathway to Haliclonacyclamine C

By analogy to the Baldwin and Whitehead proposal, we suggest a biosynthetic pathway to haliclonacyclamine C (**1.6**) (Scheme 5). In our proposal, condensation of an unsaturated dialdehyde **1.26**, a saturated dialdehyde **1.25**, two molecules of acrolein **1.12** and two molecules of ammonia produce a partially reduced bis-3-alkylpyridine macrocycle **1.27**, which sets the stage for a key intramolecular Diels-Alder cyclization leading to the natural product haliclonacyclamine C. This cyclization establishes the correct relationship between the two hydrogens on the central carbon-carbon bond linking the two piperidine rings.

Scheme 5 Proposed biosynthetic pathway to haliclonacyclamine C

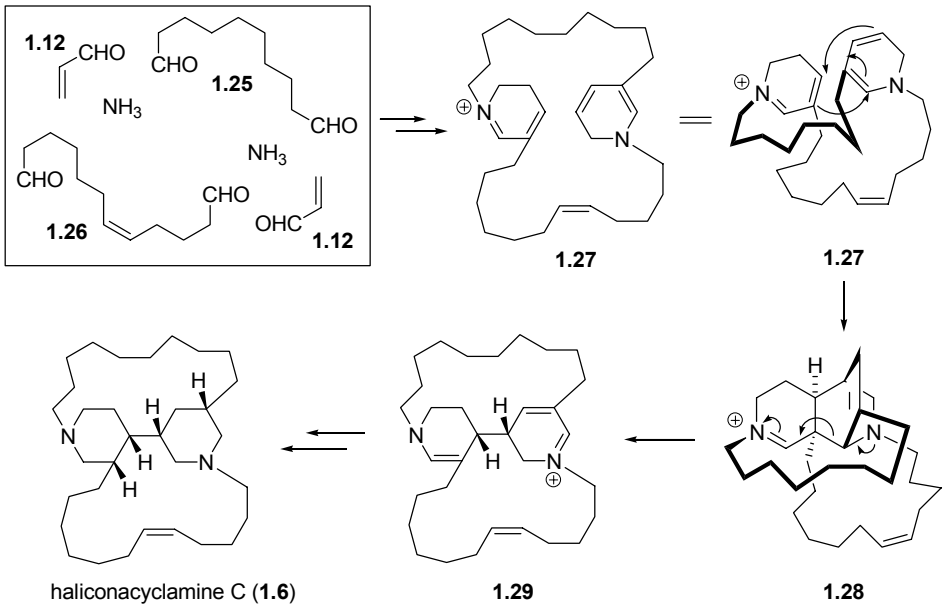

1.4 Marazano's Modification of Baldwin's Proposal

Recently, results from Marazano's laboratory have prompted them to introduce a modification of the original Baldwin's proposal for the biosynthesis of manzamine alkaloids (Scheme 6).[15,16] In their new model, they replaced acrolein unit in Baldwin's proposal with malonaldehyde **1.30**. Thus, condensation of malonaldehyde with another aldehyde and a primary amine produces the key intermediate aminopentadienal derivatives (two possible regio-isomers **1.31** and **1.32**) that have been shown[17] to be prone to cyclization to give 3-alkyl pyridinium salt **1.33**. These aminopentadienal derivatives not only produce pyridinium salts, but also could alternatively undergo a Diels-Alder cycloaddition with dihydropyridinium salt **1.34**.

Scheme 6 Marazano's modification of Baldwin's proposal

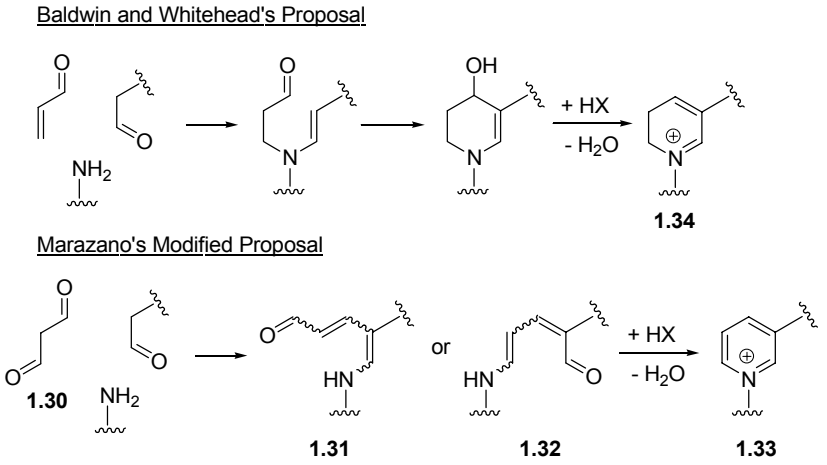

On the basis of this chemistry, Marazano and co-workers put forward a modified biogenetic pathway to the manzamine alkaloids (Scheme 7). In this new model, macrocycle **1.35**, possessing both dihydropyridinium and aminopentadienal moieties, undergoes an intramolecular Diels-Alder reaction to give cycloadduct **1.36**, an advanced intermediate in the biosynthesis of manzamine A and other biogenetically closely related marine alkaloids.

Scheme 7 Marazano's modified biogenetic pathway to manzamine A

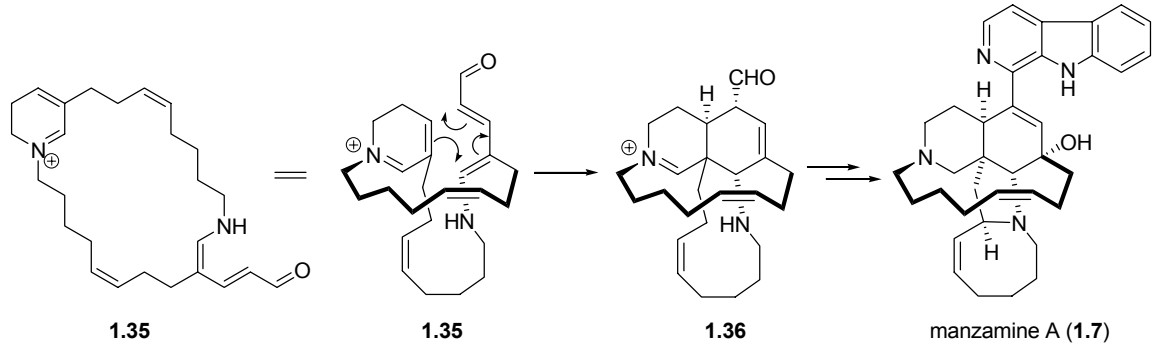

1.5 Recent Advances in the Biosynthesis of 3-Alkylpyridine

As stated above in the Background and Biological Importance section, these structurally diverse marine macrocyclic alkaloids are related to each other by a common biogenetic pathway starting from macrocycles composed of 3-alkylpyridine or reduced 3-alkylpyridine units. Therefore, the origin of the 3-alkylpyridine is one of the key issues to be addressed in the understanding of the biosynthetic pathway to these complex marine alkaloids. As already proposed by Baldwin and Whitehead in their biogenetic pathway to manzamine alkaloids, the 3-alkylpyridine motif originated from the condensation of three simple units: ammonia, a C10 unit (an unsaturated dialdehyde) and a C3 unit (acrolein) (Scheme 2). However, to date there has been no *in vivo* evidence (i.e. labeling studies) to support Baldwin's proposed biosynthetic pathway to 3-alkylpyridine, the precursor of these macrocyclic marine alkaloids including some of the most intriguing structures ever isolated from marine organisms, such as sarains and manzamines.

Most recently, Fontana and his group in Italy described the first *in vivo* evidence concerning the biosynthesis of 3-alkylpyridines in marine organisms.[18,19] They have pursued feeding experiments to elucidate a polyketide biosynthetic pathway leading to an alkylpyridine alkaloid, haminol-2 (**1.37**) (Scheme 8) which was isolated from the Mediterranean mollusc *Haminoea orbignyana*. Two preliminary experiments were carried out by feeding the mollusk *H. orbignyana* with either radio-labelled [2-^{14}C]-acetic acid and or nicotinic acid-carboxy-^{14}C and after injection, they found significant levels of radioactivity in haminol-2 (**1.37**) produced by this animal. In this way, they proved de

novo origin of haminols. In order to fully understand the biosynthesis of haminol-2 (**1.37**) in *H. orbignyana*, some other experiments were also performed by injecting the animal with either d_4-nicotinic acid ethyl ester or [1-^{13}C]-acetic acid. By means of extensive feeding experiments with ^{13}C or ^{14}C labeled acetate and nicotinic acid, and subsequent spectral studies, they proved the origin of haminol-2 (**1.37**) via a polyketide synthase (PKS) using nicotinic acid (**1.38**) as a starter unit and six molecules of acetate (or the metabolically equivalent malonate) as extender units (Scheme 8).[18] Loss of the terminal carbon of the PKS-emerging chain **1.39**, presumably due to a post-PKS decarboxylation, provides the skeleton **1.40** of haminol-2 (**1.37**). Their discovery allowed them to "conclude that haminols are produced in *H. orbignyana* through a polyketide pathway and ruled out other hypotheses about the formation of 3-alkylpyridine framework".[19] However, their studies cannot exclude that the biosynthesis of more complex marine alkaloids, such as manzamines and sarains follow other biochemical mechanisms.

Scheme 8 Proposal for the biosynthesis of **1.37** based on feeding experiments

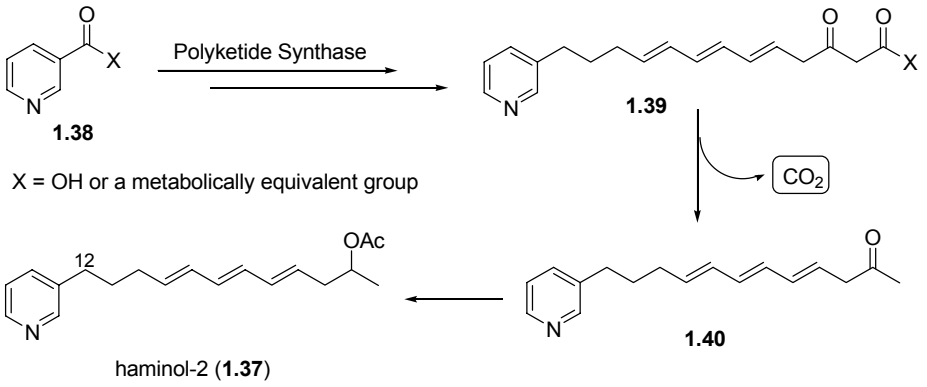

CHAPTER II

PROGRESS TOWARDS THE TOTAL SYNTHESIS OF THE TETRACYCLIC DIAMINE ALKALOID HALICLONACYCLAMINE C

2.1 Haliclonacyclamines: Isolation, Structure and Biological Activity

As discussed in Chapter I, cytotoxic alkaloids containing a 3-alkyl pyridine or piperidine motif have been frequently isolated from marine sponges. This group of marine secondary metabolites can be subdivided into tricyclic, tetracyclic or pentacyclic alkaloids. The manzamine class of alkaloids represent a complex structural variation within this group which incorporates a tetra- or pentacyclic system fused to a β-carboline unit.[20] In this chapter, we will describe progress towards the chemical synthesis of the tetracyclic haliclonacyclamine family (Figure 4).

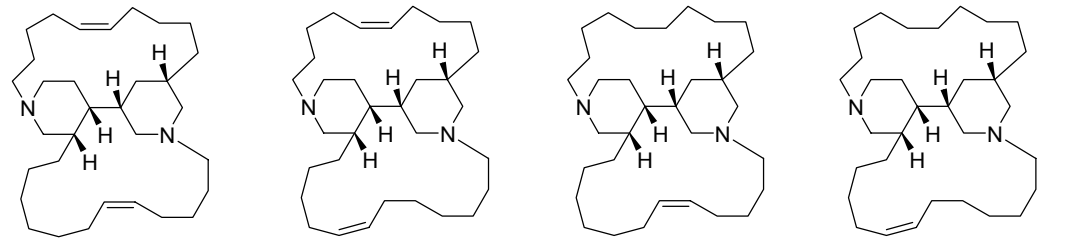

haliconacyclamine A (**2.1**) haliconacyclamine B (**2.2**) haliconacyclamine C (**2.3**) haliconacyclamine D (**2.4**)

Figure 4 Structures of haliclonacyclamines A-D

Haliclonacyclamines A (**2.1**) and B (**2.2**) were isolated from the olive-brown finger sponge *Haliclona* sp. collected at Heron Island, Great Barrier Reef in 1996 by

Garson and co-workers.[21] The same research group isolated haliclonacyclamines C (**2.3**) and D (**2.4**) from the same sponge in 1998.[20] The structures of haliclonacyclamines C and D are dihydro derivatives of haliclonacyclamines A and B respectively. Structures of the haliclonacyclamines were elucidated by extensive NMR studies and X-ray structural analysis in the case of haliclonacyclamine B (**2.2**).

The tetracyclic haliclonacyclamines show pronounced cytotoxic, antibacterial and antifungal activities. For example, haliclonacyclamine C has an IC_{50} value of 0.7 μg/mL obtained in a P_{388} assay, and also displays antibacterial activity towards *Bacillus subtilis* and strong antifungal activity against *Candida albicans* and *Trichophyton mentagrophytes*.[20]

2.2 Retrosynthetic Analysis of Haliclonacyclamine C

Although the proposed biosynthesis of haliclonacyclamine C (**2.3**) and its relationship to the biosynthesis of other related marine secondary metabolites are fascinating, we chose to engage in the synthesis of haliclonacyclamine C from a purely classical chemical approach (For a proposed biomimetic synthesis of haliclonacyclamine C see Chapter I). The common structural feature shared by this group of secondary metabolites is a reduced bis-piperidine core structure combined with two bridging macrocycles. Two examples, haliclonacyclamine C (**2.3**) and arenosclerin B (**2.5**) illustrate a common tetracyclic structural motif possessing a 3,4'-linked bis-piperidine core (Figure 5). The primary structural variations within this group of secondary metabolites occur in the stereochemistry of the core bis-piperidine structure and the

oxidation state of two bridging macrocycles. For example, haliclonacyclamine C has only one site of unsaturation while arenosclerin B has three sites of unsaturation and an allylic hydroxyl group of undefined stereochemistry located at C(22). More subtle differences in structure occur in the relative stereochemistry of stereogenic centers arranged within the bis-piperidine ring system. In the case of haliclonacyclamine C (**2.3**) and arenosclerin B (**2.5**), they share common stereochemistry at C(7) and C(9) but differ in configuration at C(2) and C(3). One of our key transformations to be addressed in the synthesis of haliclonacyclamine C is a palladium-mediated cross-coupling to generate the core bis-piperidine structure by formation of the C(3)-C(9) carbon-carbon bond. We also judge control of the four stereocenters that are incorporated within the central bis-piperidine to be synthetically challenging, particularly the relative stereochemistry of the central carbon-carbon bond that links the two piperidine units.

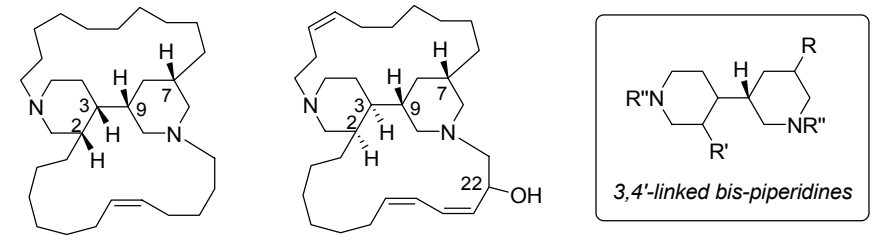

haliconacyclamine C (**2.3**) arenosclerin B (**2.5**)

Figure 5 Structures of haliclonacyclamine C and arenosclerin B

A retrosynthetic analysis of haliclonacyclamine C is shown in Figure 6. The stereoselective hydrogenation of diene **2.6** will be the key transformation to give a bis-

piperidine unit incorporating the correct relative stereochemistry common to the natural product haliclonacyclamine C (**2.3**).

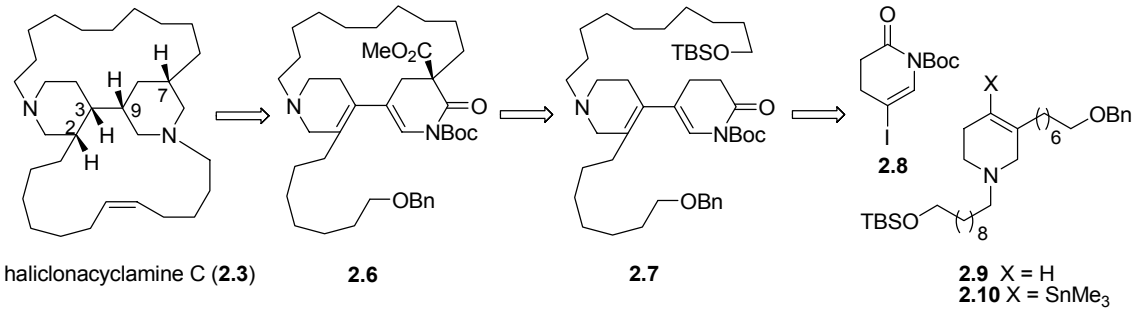

Figure 6 Retrosynthetic analysis of haliclonacyclamine C

This prediction is based on examination of molecular mechanics modeling of **2.11** (Figure 7). Using MMFF94 force field and water GB/SA solvent model in Macromodel, a Monte-Carlo global minimization of **2.11** is applied to obtain the optimized geometry. The four lowest energy conformations are shown in Figure 7. It can be clearly seen that the molecular model of **2.11** shows the macrocyclic ring effectively blocks one face of ring **B**, thus favoring hydrogenation from the other face of ring **B**. Also it should be noted that the alkyl chain on C2 in ring **B** will block the bottom face of ring **A**, thus hydrogenation will take place on the top face of ring **A**. Based on this analysis we predict the production of the relative stereochemistry found in haliclonacyclamine C. Dienes **2.6** could be synthesized from intramolecular cyclization of intermediate **2.7** (Figure 6). Palladium-mediated coupling of beta-iodo enecarbamate **2.8** and **2.9** (Heck

reaction) or **2.10** (Stille raction) would be investigated as a key reaction to construct the bis-piperidine core structure **2.7** in the total synthesis.

2.11

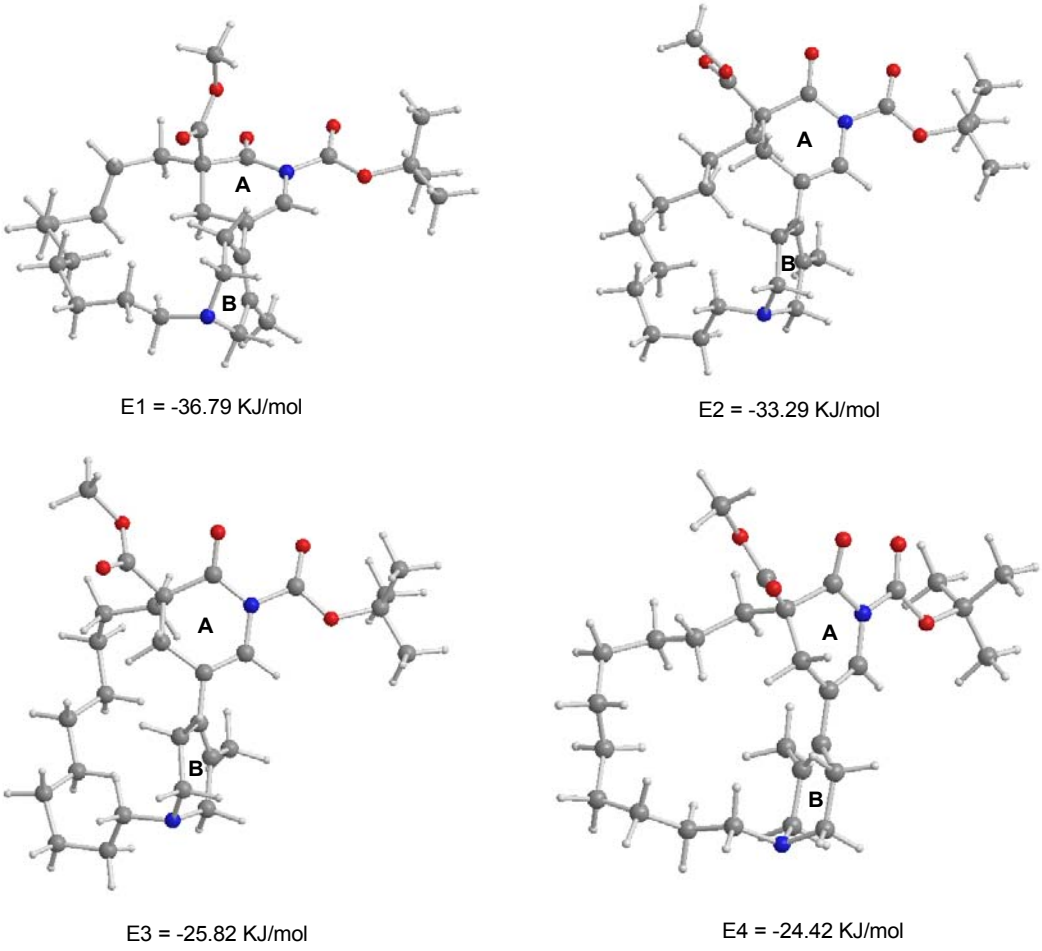

Figure 7 Molecular modeling of **2.11** (MMFF94 force field in Macromodel)

2.3 Model Study of Heck Reaction to Construct 3,4'-Linked Bis-piperidines

At the outset, we examined the Heck reaction to construct the 3,4'-linked bis-piperidines core structure. We planned to carry out the Heck reaction of beta-iodo enecarbamate **2.12** or **2.8** with olefin **2.13** to generate the core structure **2.14** of haliclonacyclamine C (Scheme 9).

Scheme 2.1 Model study of Heck reaction to construct 3,4'-linked bis-piperidines

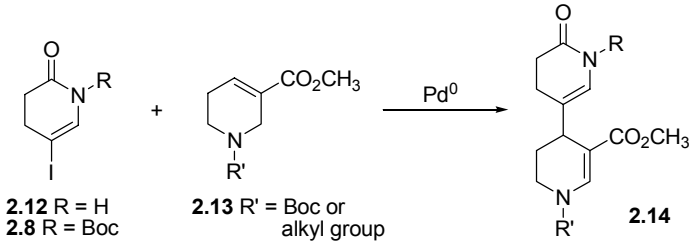

2.3.1 Mechanism of Heck Reaction

The palladium-catalyzed coupling of an aryl or vinyl halide or triflate with an alkene, known as the Heck reaction has undergone tremendous innovation since its first report in 1968.[22] It has progressed from a simple olefination of activated aryl compounds to a powerful method in organic synthesis of natural products. The catalytic cycle[23] of this reaction is outlined in Scheme 10.

Scheme 10 Mechanism of Heck reaction[23]

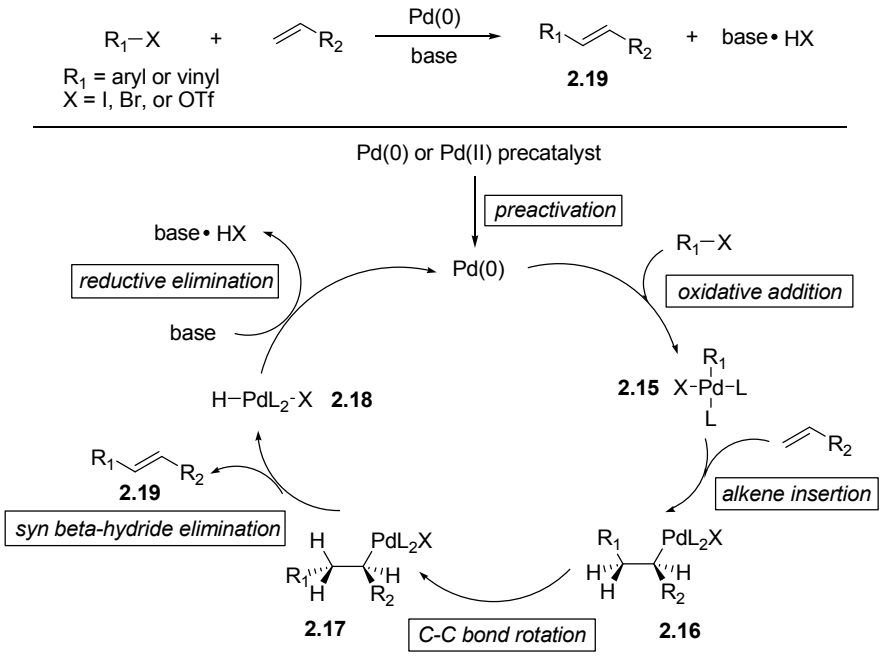

The entry into the catalytic cycle is the reduction of Pd(II) complexes to Pd(0) and the generation of active species through a preactivation step which usually includes multiple ligand exchange equilibria. Once the active Pd(0) species is formed, the oxidative addition step in the catalytic cycle takes place through insertion into an alkenyl halide or an aryl halide (R_1X) bond to give the 16-electron complex **2.15**. An insertion of the olefin into the Pd-C bond after olefin complexation with the 16-electron Pd(II) species, generates the intermediate **2.16**. This step is the product-forming step of the whole cycle, in which a new C-C bond is generated. It is noteworthy that this step is "most likely responsible for regio- and stereo- discrimination as well as substrate selectivity".[24] It also should be pointed out that the step of olefin insertion takes place as a *syn* addition and the palladium complex with bulky organic ligands is likely to be

bonded to the less hindered carbon of the olefin in order to avoid any significant steric repulsion. The next step in the Heck cycle involves a simple carbon-carbon bond rotation of **2.16** to give **2.17** which orients the palladium species and hydrogen *syn* to each other. **2.17** is ready to undergo a syn beta-hydride elimination to give the final coupling product E-alkene **2.19** and the hydridopalladium complex **2.18**. Finally, a base-induced reductive elimination of HX from **2.18** regenerates the palladium(0) catalyst, thus permitting a subsequent turn through the Heck cycle.

2.3.2 Synthesis of Beta-Iodo Enecarbamate

With the Heck route to the halicolonacyclamines in mind, we set as our first goal the synthesis of beta-iodo enecarbamates **2.12** and **2.8** (Scheme 11). Endocyclic enamides and enecarbamates are important building blocks for the synthesis of alkaloids. Generally, two approaches have been explored starting from either lactams or saturated amines. In one approach, enamides and enecarbamates can be produced from lactams via a two-step reduction and dehydration sequence.[25-27] More recent reports describe the conversion of lactams into enol triflate or phosphates that undergo Stille or Suzuki cross-coupling reactions. However, we were encouraged by a more economical and easily scaleable process, that is anodic methoxylation of lactams[28] followed by acid-catalyzed elimination of methanol. For example, electrochemical methoxylation of valerolactam **2.20** afforded aminal **2.21** in 50% overall yield (Scheme 11). The iodo group was then introduced into the beta position to afford **2.12** using a two-step procedure. Boc protection of **2.12** gave N-protected beta-iodo enecarbamate **2.8** in moderate yield.

Scheme 11 Synthesis of beta-iodo enecarbamate

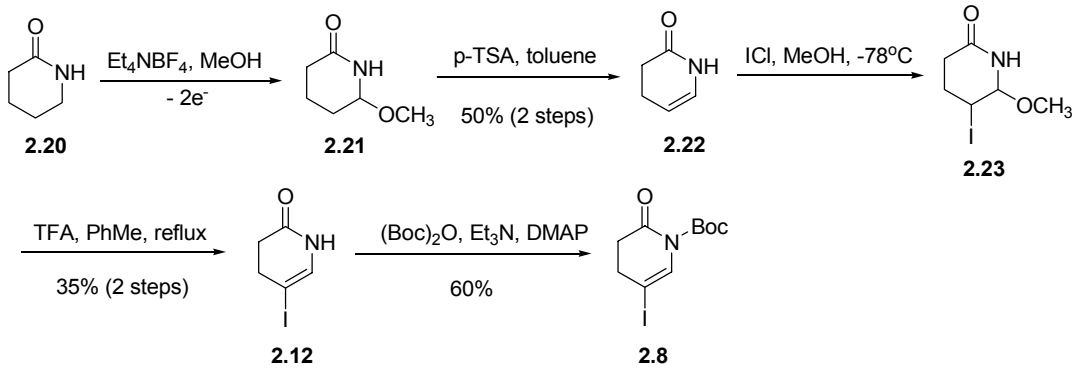

2.3.3 First Attempt to Construct 3,4'-Linked Bis-piperidines by Heck Reaction

With beta-iodo enecarbamates **2.12** and **2.8** in hand, we were ready to investigate the Heck reaction to construct the core structure 3,4'-linked bis-piperidines. The synthesis of the olefin partner **2.28** of the Heck reaction is outlined in Scheme 12. Conversion of alcohol **2.24** to amine **2.25** by applying a two-step reaction sequence proceeded in almost quantitative yield.[29] Double Michael addition of amine **2.25** to methyl acrylate generated an intermediate diester which was treated with base NaHMDS leading to a Dieckman cyclization and providing beta-keto ester **2.26**. The latter was reduced by sodium borohydride to yield beta-hydroxy ester **2.27**. A two-step dehydration reaction sequence completed the synthesis of enoate **2.28** in 81% yield.

Scheme 12 Synthesis of enoate **2.28**

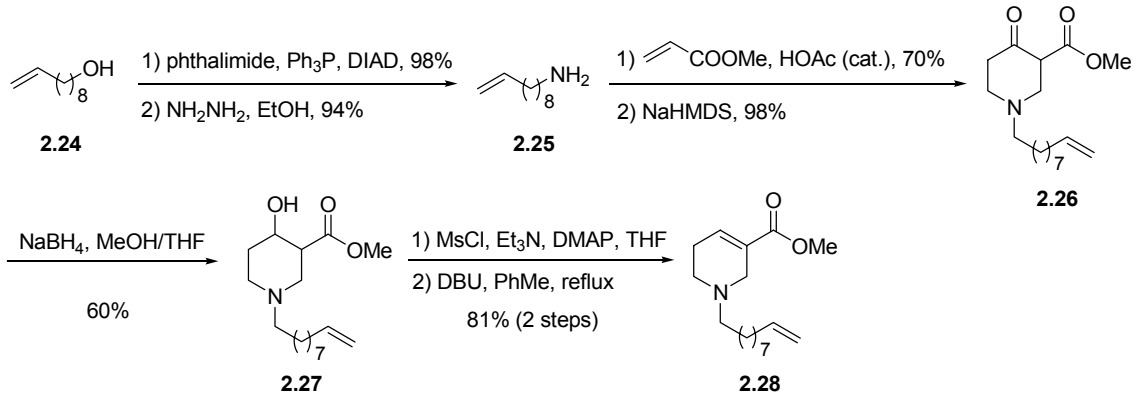

At this stage, we were ready to attempt our palladium-mediated C-C bond formation of enoate **2.28** with either vinyl iodide **2.12** or **2.8**. Unfortunately, as seen in Table 1, our attempts to construct the central C-C bond by Heck reaction failed to produce any of the desired product **2.29**. Frequently, only the isolation of starting materials was observed.

Table 1 Heck reaction of vinyl iodide with enoate **2.28**

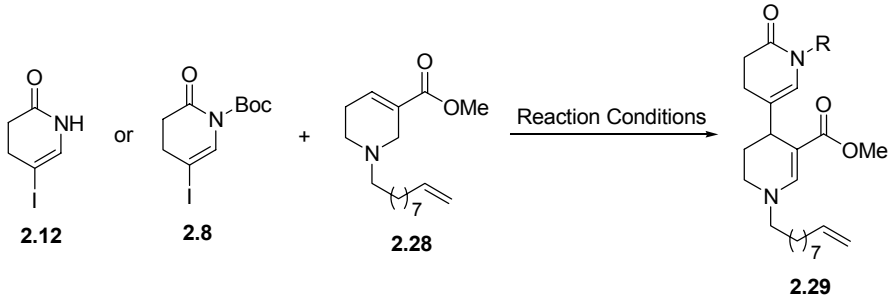

2.12 **2.8** **2.28** **2.29**

Entry	Vinyl Iodide	Catalyst	Ligand / Additive	Solvent	Temp (^oC)	Result
1	**2.12**	$Pd(OAc)_2$	PPh_3, Na_2CO_3	DMF	60	**2.12** decomposed, **2.28** recovered
2	**2.12**	$Pd(OAc)_2$	PPh_3, Et_3N	THF	25	**2.12** patially decomposed, **2.28** recovered
3	**2.12**	$Pd(OAc)_2$	PPh_3, Ag_2CO_3	CH_3CN	60	**2.12** decomposed, **2.28** recovered
4	**2.8**	$Pd_2(dba)_3$	BINAP, Ag_2CO_3	DMA	80	Unknown compound
5	**2.8**	$Pd_2(dba)_3$	dppe, Et_3N	CH_3CN	80	**2.8** and **2.28** recovered
6	**2.8**	$Pd(OAc)_2$	$NaHCO_3$, n-Bu_4NCl, 4A MS	DMF	60	**2.8** decomposed, **2.28** recovered

Interestingly, when we replaced vinyl iodide **2.12** or **2.8** with iodobenzene (Scheme 13), the Heck reaction did proceed to give coupled product **2.30** under Jeffery's condition[30]. However, **2.30** was not the product we desired. Instead of reacting with the enoate alkene, iodobenzene reacted with the terminal olefin of **2.28** to give undesired coupled product **2.30**.

Scheme 13 Heck reaction of iodobenzene with enoate **2.28**

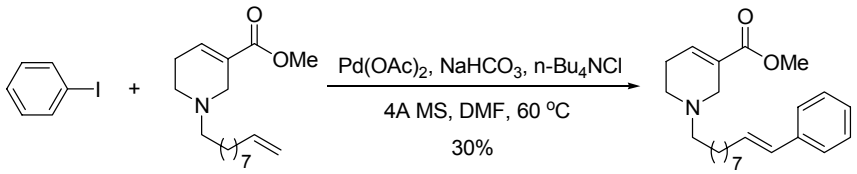

2.28 **2.30**

In order to test the reactivity of the beta-iodo enecarbamate partner **2.8**, we conducted a model study on the Heck reaction of **2.8** and ethyl acrylate. It was found that under Jeffery's condition,[30] the Heck coupled product **2.31** was generated in good yield (Scheme 14). At this stage, we were confident that the oxidative addition of active Pd(0) species to the carbon-iodine bond did take place, which is the first step in the Heck catalytic cycle.

Scheme 14 Heck reaction of beta-iodo enecarbamate **2.8** and ethyl acrylate

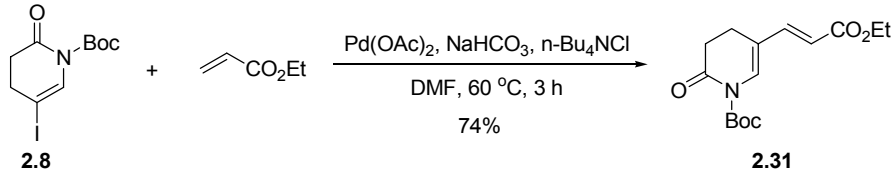

2.8 **2.31**

2.3.4 Second Attempt to Construct 3,4'-Linked Bis-piperidines by Heck Reaction

Since the reactivity of the beta-iodo enecarbamate proved not to be a problem from our model study (Scheme 14), we reasoned that the failure is due to the electron-rich terminal olefin competing with the electron-deficient enoate olefin within the piperidine ring in the olefin insertion step in the Heck catalytic cycle (Scheme 10). We therefore chose to examine enoate **2.36**, which has no other sites of unsaturation. The synthesis began with Boc protection of 4-piperidone **2.32** to give **2.33**, which was treated with LHMDS followed by quenching with methyl cyanoformate (Mander's reagent) to generate beta-keto ester **2.34** (Scheme 15). Enoate **2.36** was obtained in good yield by

using a three-step reaction sequence we developed in the synthsis of enoate **2.28** (Scheme 12).

Scheme 15 Synthesis of enoate **2.36**

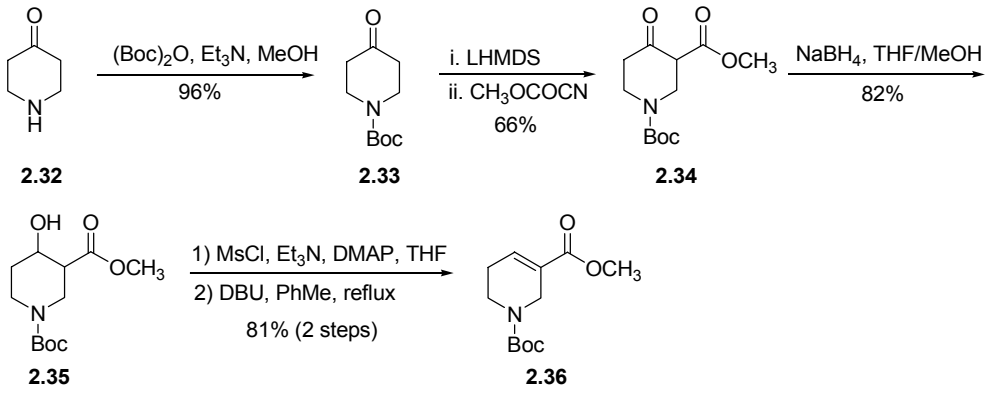

To our delight, Heck coupling of iodobenzene and the modified olefin **2.36** proceeded to give the desired product **2.37** under Jeffery's condition (Scheme 16). However, under a variety of reaction conditions, beta-iodo enecarbamate **2.8** failed to couple with olefin **2.36**. The lack of reactivity of this Heck reaction is probably due to the steric hindrance of the tri-substituted olefin partner, which makes it difficult to undergo olefin insertion to the R-Pd-I complex, the product-forming step in the Heck catalytic cycle (Scheme 10).

Scheme 16 Heck reaction of olefin **2.36**

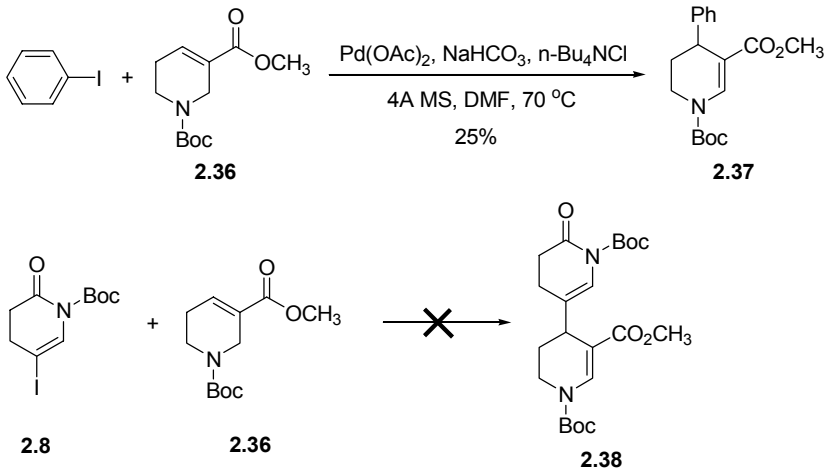

2.4 Model Study of Stille Coupling to Construct 3,4'-Linked Bis-piperidines

We now turn our attention to the application of Stille coupling to construct the core structure 3,4'-linked bispiperidines (Scheme 17).

Scheme 17 Model study of Stille coupling to construct 3,4'-linked bis-piperidines

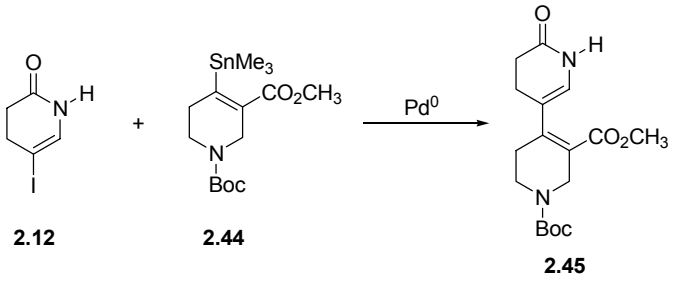

2.4.1 Mechanism of Stille Coupling

Alkenyltins undergo a palladium-mediated coupling with a wide variety of organic halides and triflates. The high yields and mild reaction conditions of this

reaction have been led to much success in natural product synthesis. An additional virtue of this palladium-mediated coupling reaction is that a variety of functional groups (e.g. CO_2R, CN, OH) can be tolerated. A catalytic cycle of the so-called Stille cross-coupling is described in Scheme 18.[23] In the catalytic cycle, a coordinatively unsaturated 14-electron palladium(0) complex is generated as the catalytically active species. The first step in the catalytic cycle is an oxidative addition of the organic eletrophile R-X to the palladium(0) catalyst leading to a 16-electron palladium(II) complex **2.40**. Then **2.40** participates in a transmetalation step with the organotin reagent R_1-$Sn(R_2)_3$ to give a new palladium complex **2.41**. After facile isomerization of *trans* isomer **2.41** to *cis* isomer **2.42**, a reductive elimination releases the cross-coupled product R-R_1 and regenerates the active palladium(0) complex allowing for another catalytic cycle.

Scheme 18 Mechanism of Stille coupling[23]

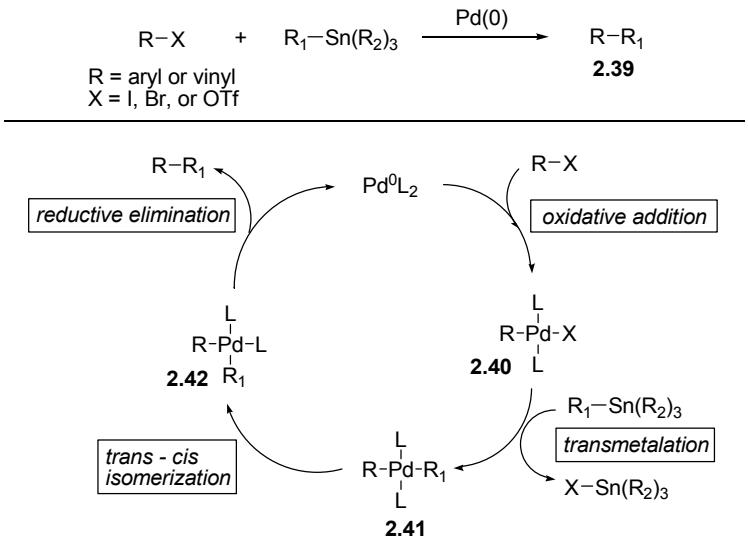

2.4.2 Synthesis of Vinyl Stannane 2.44

The synthesis of Stille coupling reaction partner vinyl stannane **2.44** started from beta-keto ester **2.34** (Scheme 19). Treatment of **2.34** with base KHMDS followed by the addition of Comins' reagent[31] generated the vinyl triflate **2.43** in excellent yield. Conversion of vinyl triflate **2.43** to vinyl stannane **2.44** under Wulff conditions[32] (Me_6Sn_2, $Pd(PPh_3)_4$, LiCl, THF) did not afford any desired product. To our delight, higher-order stannyl cuprate[33] addition to the vinyl triflate furnished vinyl stannane **2.44**.

Scheme 19 Synthesis of vinyl stannane **2.44**

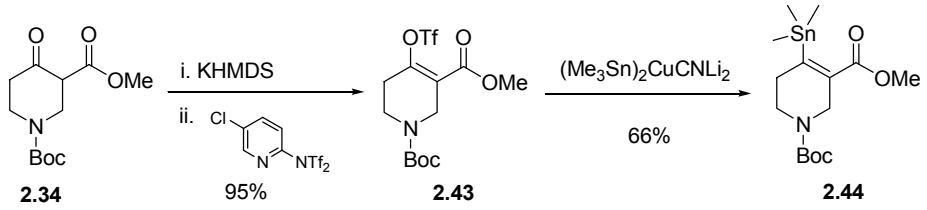

2.4.3 Stille Coupling to Construct 3,4'-Linked Bis-piperidine Core Structure

Next, we turned our attention to the Stille coupling of the two components **2.44** and **2.12**. It has been well-known that a major limitation of Stille coupling reactions arises from steric hinderance, especially in the vinyl stannane component. So there was some concern regarding the steric congestion of the vinyl stannane **2.44**. Indeed, our initial attempts to construct the central C-C bond by traditional Stille cross-coupling conditions either failed to produce any of the desired diene **2.45** (Scheme 20) or did not afford significant quantities of the desired product. At this juncture, we were intrigued

by a report from Corey and co-workers detailing the superiority of using CuCl rather than other Cu(I) salts as an additive in the Stille cross-coupling reaction of vinyl/aryl halides or triflates.[34] We were pleased to find that implementation of the Corey procedure (rigorous exclusion of oxygen and moisture) resulted in smooth conversion of vinyl stannane **2.44** to the desired diene **2.45** in good yield as illustrated in Scheme 20. It is believed that the function of CuCl is to convert the vinylstannane to a more reactive vinylcopper(I) species, thus to facilitate the transmetallation step in the catalytic cycle of Stille coupling reactions.

Scheme 20 Stille coupling of **2.12** and **2.44**

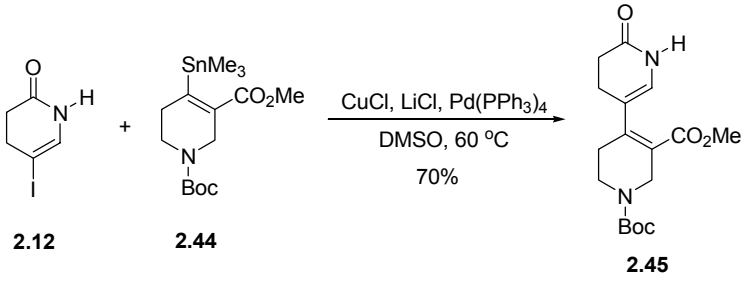

2.12 **2.44** **2.45**

2.4.4 Stereoselective Hydrogenation of Diene 2.45

Pleased with our ability to obtain diene **2.45** in synthetically useful amounts, we now turned our attention to establishing the requisite stereochemistry across the central C-C bond by a heterogeneous hydrogenation as illustrated in Scheme 21. In principle, there are four possible diastereomers produced from the reduction of **2.45**. The 500 MHz ^{1}H-NMR spectrum of the hydrogenation product **2.46** was not well resolved (Figure 8), perhaps due to isomers as well as rotamers originating from the Boc group on the

nitrogen. Interestingly, when we analyzed the hydrogenated product **2.46** using Gas Chromatography (GC), only one product was indicated.

Scheme 21 Hydrogenation of diene **2.45**

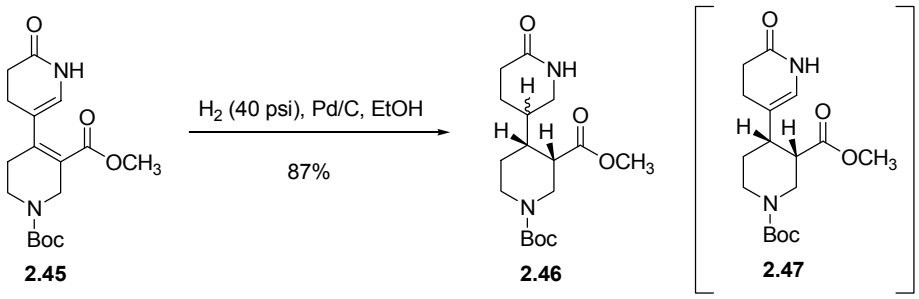

To our delight, when we applied the method of VT-NMR (75 ^{o}C, solvent: $(CD_3)_2SO$) to analyze the compound, the spectrum clearly showed the hydrogenated product **2.46** coalescent to a single diastereomer (Figure 8). It is also noteworthy that when running the hydrogenation of diene **2.45**, we did isolate a byproduct that we believe was the partially reduced product **2.47** (Scheme 21). In this case, we were a little surprised that the tetra-substituted olefin was more easily reduced than the tri-substituted olefin.

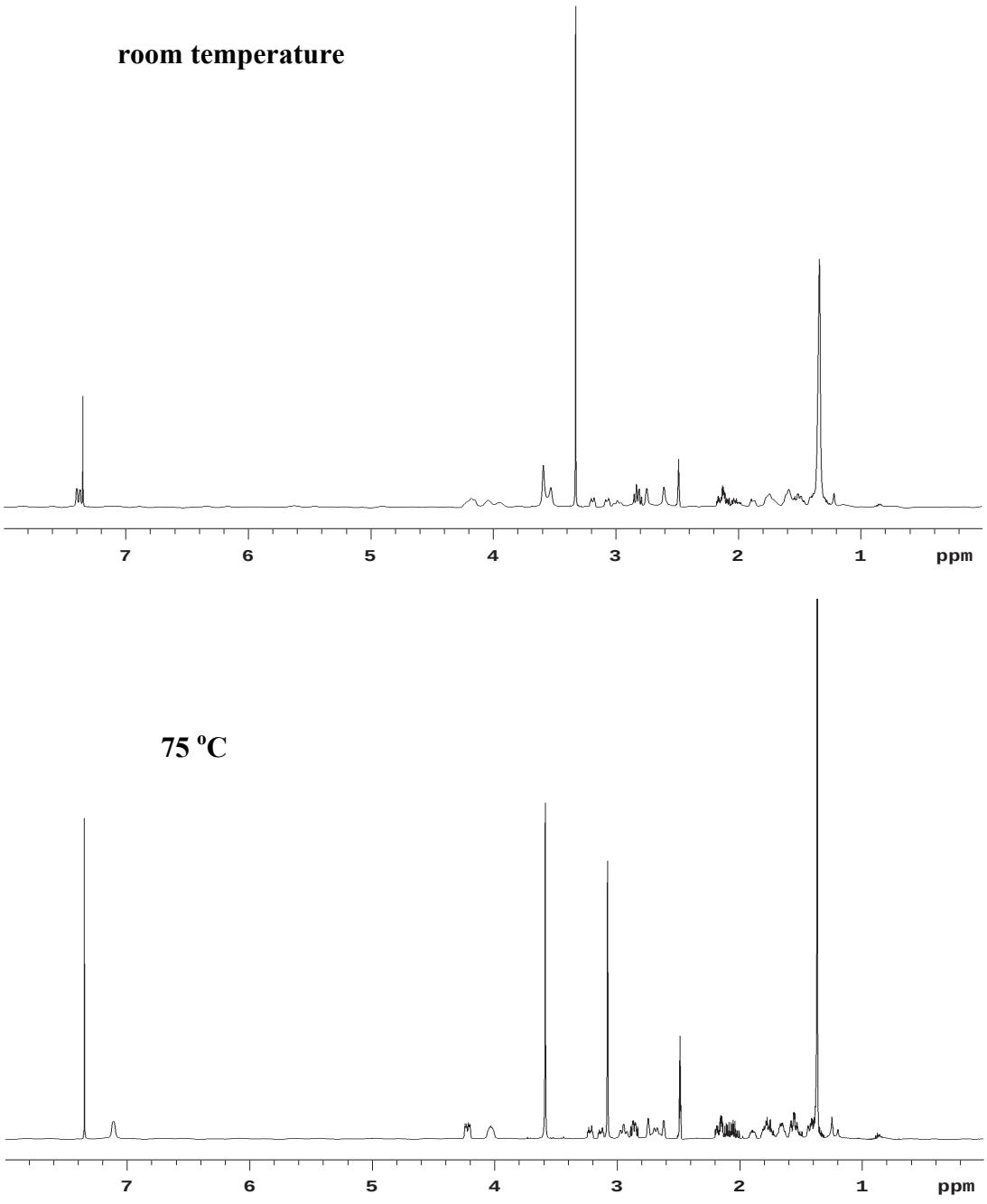

Figure 8 Comparison of room temperature and 75 ^{o}C ^{1}H-NMR of **2.46** in $(CD_3)_2SO$

Conformational analysis of partially reduced product **2.47** by molecular modeling in macromodel (MMFF94 force field, water GB/SA model) is shown in Figure 9. The lowest energy conformation from calculation is E1, which energy is -316.66 KJ/mol. Figure 9 also shows the next three lowest energy conformations E2, E3 and E4 for comparison. From the molecular modeling of **2.47**, we can clearly see that the methyl ester group blocks one face of ring A (Figure 9), thus hydrogenation presumably takes place from the other face of ring A to generate one single diastereomer.

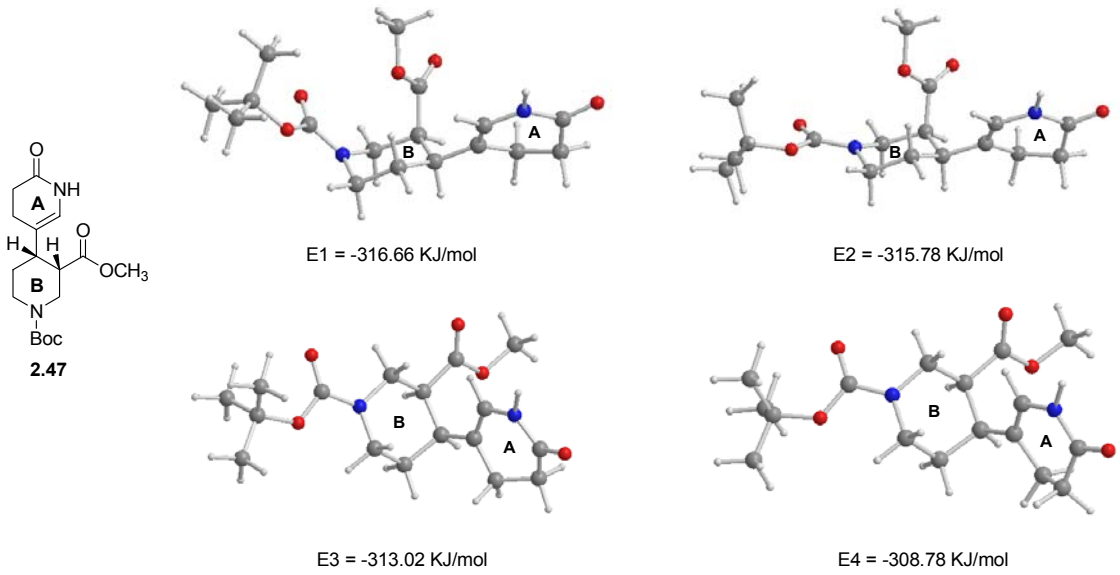

Figure 9 Molecular modeling of **2.47** (MMFF94 force field in Macromodel)

Based on the above molecular modeling analysis, we predict the hydrogenation product to be **2.48** (Scheme 22), the diastereomer of the product **2.49** that we desire.

Scheme 22 Predicted hydrogenation product of diene **2.45**

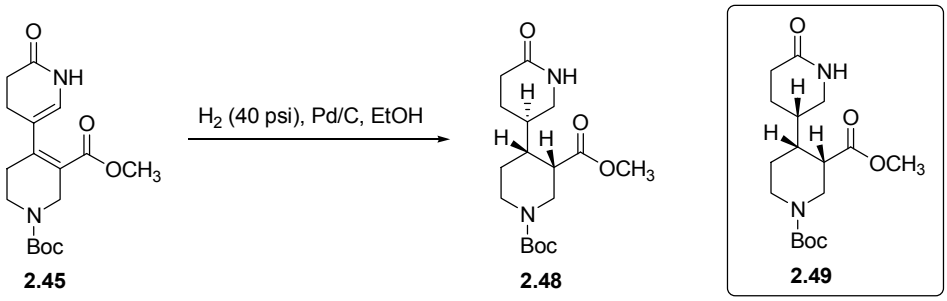

In order to determine the relative stereochemistry of the hydrogenation product **2.46** (Scheme 21), we planned to make crystal derivative of **2.46** and confirm the stereochemistry by single crystal X-ray analysis of the derivative. We attempted to funtionalize the lactam nitrogen of **2.46** with aromatic groups that would impart crystallinity. Unfortunately, as seen in Table 2, protection of the nitrogen with 2,4-dinitrobenzenesulfonyl chloride using several bases did not furnish any desired product **2.50**. When we used the less hindered *p*-toluenesulfonyl chloride to protect the lactam nitrogen, it still did not yield any desired product. We were pleased to find that protection of **2.46** with 4-bromobenzoyl chloride using sodium hydride as a base gave the desired product in good yield. Unfortunately this derivative is not a crystal that can be used for single crystal X-ray analysis.

Table 2 Protection of lactam nitrogen of **2.46**

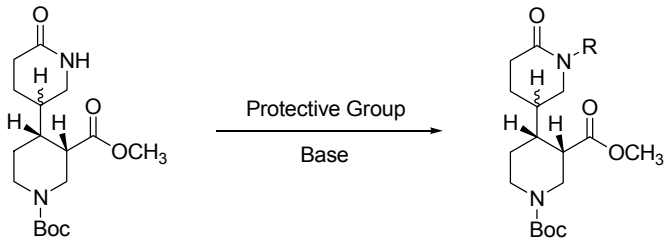

2.46 **2.50**

Entry	Protective Group	Base	Result
1	2,4-dinitrobenzenesulfonyl chloride	NaH	no desired product **2.50**
2	2,4-dinitrobenzenesulfonyl chloride	n-BuLi	no desired product **2.50**
3	2,4-dinitrobenzenesulfonyl chloride	NaHMDS	no desired product **2.50**
4	*p*-toluenesulfonyl chloride	NaHMDS	no desired product **2.50**
5	4-bromobenzoyl chloride	NaH	68% yield of product **2.50**, not crystal

Now we have turned our attention to making crystal derivative of hydrogenation product **2.46** via reduction of the methyl ester to a primary alcohol followed by protection of both nitrogen and oxygen with protective groups (Scheme 23). The assignment of relative stereochemistry of **2.46** via experiment is currently under investigation. Once we are able to generate a crystalline derivative of **2.46**, we will examine our stereochemical prediction of the hydrogenation product **2.46** based on our molecular modeling studies. We believe that it is important for us to understand the reason for stereoselective hydrogenation of the diene in terms of future synthetic studies towards the total synthesis of this family of macrocyclic diamine alkaloids.

Scheme 23 Future work on making crystal derivative of **2.46**

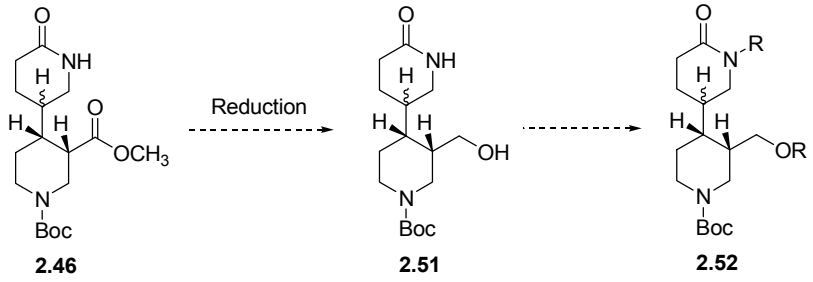

2.46 **2.51** **2.52**

2.5 Future Directions

Currently, our efforts are directed towards the synthesis of vinyl stannane **2.10** as depicted in Figure 10 by applying the chemistry we have developed for the synthesis of **2.26** (Scheme 12) and **2.44** (Scheme 19). Once we obtain vinyl stannane **2.10**, we will couple it with beta-iodo enecarbamate **2.11** to give the coupled product **2.8** as described in Figure 6. Since we have developed a general methodology for the preparation of 3,4'-linked bis-piperidines, work on this project will continue along these lines with the focus on stereoselective hydrogenation of the corresponding diene **2.6** (Figure 6) to generate the reduced bis-piperidines incorporating the requisite stereochemistry.

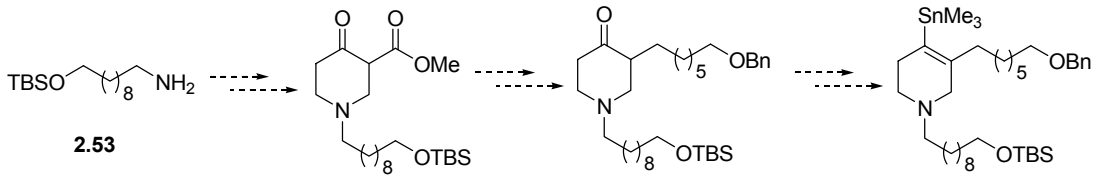

2.53 **2.54** **2.55** **2.10**

Figure 10 Synthetic approach to vinyl stannane **2.10**

We also examined the conformation of diene **2.45** and compared the dihedral angle of C(2)-C(3)-C(9)-C(10) to that in **2.11**. The conformations of **2.45** and **2.11** were obtained by a Monte-Carlo global minimization of **2.45** using MMFF94 force field and water GB/SA solvent model in Macromodel (Figure 11). The dihedral angle of C(2)-C(3)-C(9)-C(10) in **2.11** is 85^{o}, while the same dihedral angle in **2.45** is 66^{o}. Since we have obtained one single diastereomer from the hydrogenation of diene **2.45**, we are confident in our ability to generate only one diastereomer out of the hydrogenation of diene **2.11**. Although we presumably obtained the diastereomer **2.48** with the stereochemistry opposite to what we desire in the hydrogenation of diene **2.45** based on our molecular modeling studies, we believe that with the macrocycle tethered the two piperidine rings and long alkyl chain sitted in the C(2) position, we will be able to obtain the desired stereoselective hydrogenation product as we have discussed in the section of Retrosynthetic Analysis of Haliclonacyclamine C in this chapter.

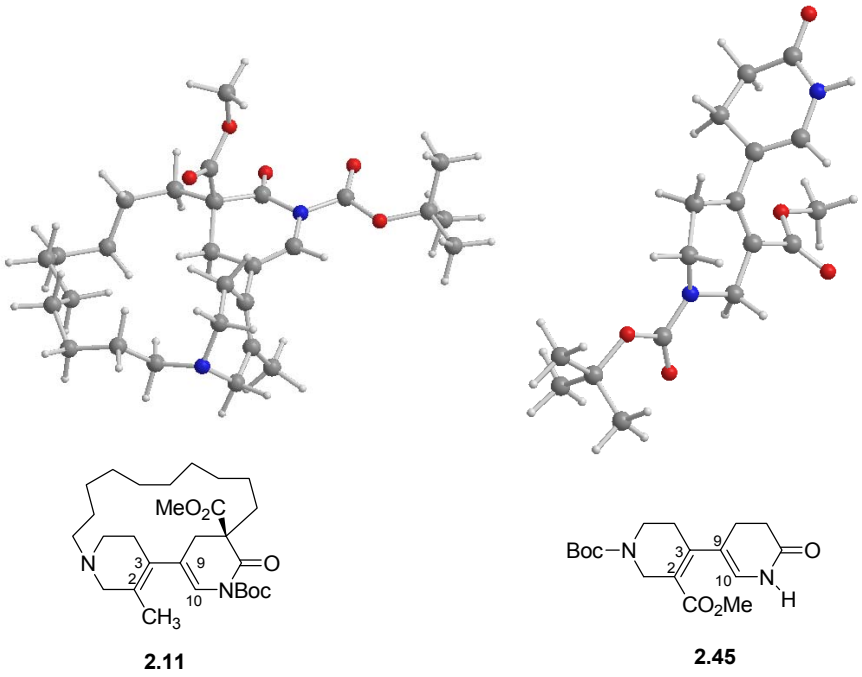

Figure 11 Molecular modeling of **2.11** and **2.45** (MMFF94 force field in Macromodel)

2.6 Experimental Section

General Procedures. Reagents were obtained from commercial suppliers, and where appropriate were purified prior to use. All reactions were carried out under a nitrogen or argon atmosphere using dry glassware which had been flame-dried under vacuum and back filled with argon, unless otherwise noted. All necessary solvents were purified prior to use. Tetrahydrofuran and ethyl ether were distilled from sodium/benzophenone; dichloromethane and benzene were distilled from calcium hydride. Triethylamine was distilled from calcium hydride and stored over sodium hydroxide. Reactions were monitored by thin-layer chromatography (TLC) using 0.25-

mm E. Merck precoated silica gel plates. Visualization was accomplished with UV light and aqueous ceric ammonium molybdate solution, anisaldehyde stain, or potassium permanganate stain followed by charring on a hot-plate. Flash chromatography was performed using silica gel 60 (particle size 230-400 mesh) with the indicated solvent. Yields refer to chromatographically and spectroscopically pure compounds unless otherwise noted. Melting points are uncorrected unless otherwise noted. ^{1}H and ^{13}C NMR spectra were recorded on Varian 500 MHz spectrometers at ambient temperature, unless otherwise noted. ^{1}H and ^{13}C NMR data are reported as δ values relative to tetramethylsilane, chloroform, or DMSO. High-resolution mass spectra were obtained at Texas A&M University Mass Spectrometry Service Center by Dr. Shane Tichy on an API QSTAR Pulsar Instrument.

Molecular modeling studies of compounds **2.11**, **2.45** and **2.47** were performed in Macromodel using Monte-Carlo global minimization and MMFF94 force field. Water GB/SA model and 1000 steps of structural minimization were applied.

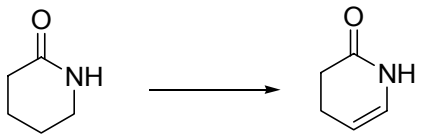

2.20 **2.22**

Enamine 2.22. Valerolactam **2.20** (3.40 g, 34.3 mmol) and tetraethylammonium tetrafluoroborate (3.0 g, 13.8 mmol) were added to methanol (100 mL). The reaction vessel was equipped with one graphite-rod anode and one graphite-rod cathode, and a magnetic stirring bar. During the electrolysis, the voltage was 25 V and the current was about 0.7 A. After stirring the reaction at room temperature for 11 h, GC analysis showed the starting material disappeared. The reaction was poured into a mixture of diethyl ether (50 mL) and pentane (50 mL). The mixture was filtered, and concentrated *in vacuo* to get the crude product **2.21**. To a solution of the above crude product **2.21** in toluene (100 mL) was added p-toluenesulfonic acid (0.1 g, cat.). The reaction mixture was refluxed for 2 h using a Dean-Stark trap. The solution was then cooled and the solvent was removed *in vacuo*. The residue was purified by flash column chromatography (3:1 hexanes/EtOAc) to afford 1.66 g (50%, over 2 steps) of enamine **2.22** as a white solid. Spectral data correlated with the reported values[35].

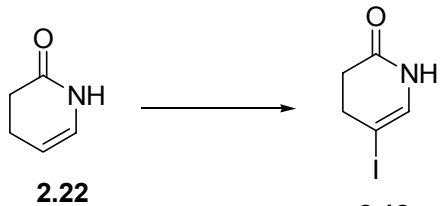

2.22 **2.12**

Beta-iodo Enamine 2.12. To a sitirred solution of **2.22** (3.64 g, 37.5 mmol) in methanol (100 mL) at -78 ^{o}C was added dropwise ICl (0.8 M solution in CH_2Cl_2, 70.4 mL, 56.3 mmol). The resulting yellow suspension was stirred at -78 ^{o}C for 1 h, after which a saturated aqueous solution of $Na_2S_2O_3$ (50 mL) was added and stirring continued for an additional 30 min. The mixture was extracted with Et_2O (3 X 50 mL). The combined organic extracts were washed with brine, dried over $MgSO_4$, filtered and concentrated *in vacuo* to give a crude product **2.23** as a yellow oil.

To a stirred room temperature solution of the above crude product **2.23** in toluene (200 mL) was added trifluoroacetic acid (0.091 mL). The reaction flask was immediately lowered into a preheated 145 ^{o}C oil bath. The solution was refluxed for 10 min during which time the solution turned a dark red color. The reaction flask was cooled to room temperature and transferred to an ice bath. When the internal temperature reached room temperature, triethylamine (0.2 mL) was added and the solvent was removed *in vacuo*. The residue was purified by flash column chromatography (4:1 hexanes/EtOAc) to afford 2.92 g (35%, over 2 steps) of enamine **2.12** as a light yellow solid. IR (neat) 3447 broad, 3201, 3088, 2930, 1670, 1644 cm^{-1}; ^{1}H-NMR (500 MHz, $CDCl_3$) δ 8.29 (s broad, 1H), 6.44 (dt, J = 4.5, 1.5 Hz, 1H), 2.72 (t, J = 8.0 Hz, 2H), 2.55 (t, J = 7.5 Hz, 2H); ^{13}C-NMR

(125 MHz, $CDCl_3$) δ 170.0, 130.9, 68.1, 33.0, 31.7; HRMS (ESI) *m/z* 229.9642 $[(M+Li)^+$ calculated for C_5H_6INOLi: 229.9654].

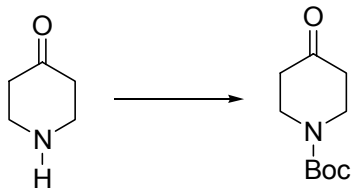

2.32 **2.33**

Ketone 2.33. To a stirred solution of triethylamine (4.52 mL, 32.5 mmol) in MeOH (25 mL) was added 4-piperidone monohydrate hydrochloride **2.32** (1.00 g, 6.49 mmol) and di-*tert*-butyl dicarbonate (4.48 mL, 19.5 mmol). The reaction mixture was heated at 45 ^oC for 1.5 h, the solvent was evaporated *in vacuo*. 2N HCl (10 mL) and ethyl acetate (20 mL) were added. The two phases were separated and the aqueous phase was extracted with EtOAc (3 X 10 mL). The combined organic extracts were dried over $MgSO_4$ to give, after evaporation of the solvent, 1.29 g (100%) of pure ketone **2.33** as a white solid. Spectral data correlated with the reported values.[36]

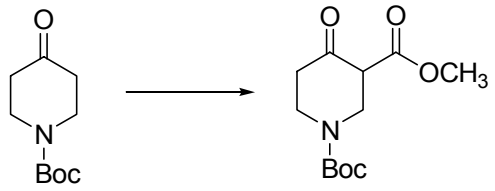

2.33 **2.34**

Beta-keto Ester 2.34. To a stirred solution of LHMDS (1.73 mL of 1.0M solution in tetrahydrofuran, 1.73 mmol) in tetrahydrofuran (8 mL) at –78 ^{o}C was added was added ketone **2.33** (0.200 g, 1.51 mmol) in tetrahydrofuran (7 mL) dropwise via cannula. The reaction was stirred at –78 ^{o}C for 30 min and then quenched with H_2O (15 mL). The two phases were separated and the aqueous phase was extracted with EtOAc (3 X 10 mL). The combined organic extracts were dried over $MgSO_4$, filtered, and concentrated *in vacuo*. The residue was purified by flash column chromatography (15:1 hexanes/EtOAc) to afford 0.170 g (66%) of beta-keto ester **2.34** as a colorless oil. Spectral data correlated with the reported values.[37]

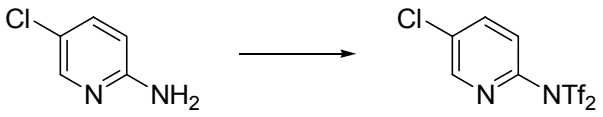

N-(5-chloro-2-pyridyl)triflimide.[38] To a clear solution of 2-amino-5-chloropyridine (8.0 g, 62.2 mmol) in CH_2Cl_2 at -78 ^{o}C was added pyridine (10.6 mL, 130.6 mmol). Then a solution of triflic anhydride (22.0 mL, 130.6 mmol) in CH_2Cl_2 (50

mL) was added dropwise via addition funnel over 3-4 hours at -78 ^{o}C. The reaction was stirred at –78 ^{o}C for 2 hours, then the cooling bath was removed and stirring was continued at room temperature for 19 hours. The reaction mixture was quenched with cold H_2O (20 mL) and the layers were separated. The aqueous phase was extracted with CH_2Cl_2 (3 X 20 mL). The combined organic extracts were washed with 10% NaOH solution (60 mL), cold H_2O (40 mL), brine (40 mL) and dried over $MgSO_4$. After filtration, the solvent was removed under vacuum to give the crude product. Vacuum distillation of crude product gave 20.2 g of pure N-(5-chloro-2-pyridyl)triflimide (b.p. 90-95 ^{o}C/1.5 mmHg) as a white solid. Spectral data correlated with the reported values[38].

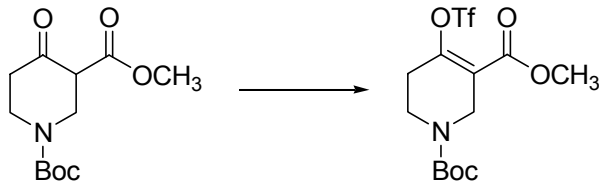

2.34 **2.43**

Vinyl Triflate 2.43. To a solution of beta-keto ester **2.34** (0.256 g, 0.996 mmol) in tetrahydrofuran (6 mL) at –78 ^{o}C was added KHMDS (2.39 mL of 0.5M solution in toluene, 1.20 mmol). The reaction mixture was warmed to –20 ^{o}C during a period of 2 h, then cooled the reaction mixture down to –78 ^{o}C and a solution of N-(5-chloro-2-

pyridyl)triflimide (0.470 g in 3 mL tetrahydrofuran) was added. The reaction continued stirring for 24 h in the process warming to room temperature. The reaction was concentrated *in vacuo*. The residue was purified by flash column chromatography (10:1 hexanes/EtOAc + 1% Et_3N) to afford 0.368 g (95%) of vinyl triflate **2.43** as a colorless oil. IR (neat) 2976, 1706, 1424, 1245, 1209 cm^{-1}; ^{1}H-NMR (500 MHz, $CDCl_3$) δ 4.27 (s, 2H), 3.83 (s, 3H), 3.62 (t, J = 5.5 Hz, 2H), 2.51 (m, 2H), 1.48 (s, 9H); ^{13}C-NMR (125 MHz, $CDCl_3$) δ 162.8, 153.9, 122.0, 119.5, 116.9, 114.4, 81.0, 52.3, 43.0, 39.3, 28.8, 28.3; HRMS (ESI) *m/z* 390.0804 [$(M+H)^+$ calculated for $C_{13}H_{19}O_7F_3NS$: 390.0834].

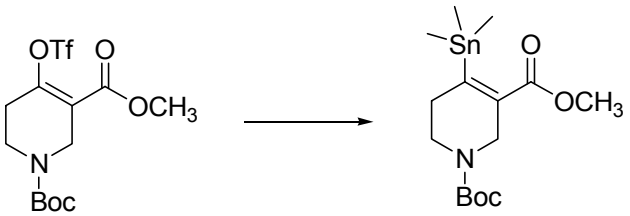

2.43 **2.44**

Vinyl Stannane 2.44. Methyllithium (0.419 mL of 1.6 M solution in diethyl ether, 0.670 mmol) was added dropwise to a solution of hexamethylditin (0.804 mL of 1.0 M solution in tetrahydrofuran, 0.804 mmol) in tetrahydrofuran (5 mL) at -30 ^oC under argon. The reaction mixture was stirred at -30 ^oC for 30 min. Then the reaction was cooled to -65 ^oC and CuCN (0.030 g, 0.335 mmol) was added in the solid form. The reaction mixture turned to a green-yellow solution.

To a solution of vinyl bromide **2.43** (0.100 g, 0.258 mmol) in tetrahydrofuran (5 mL) at –65 ^{o}C was added a solution of the higher order cuprate $(Me_3Sn)_2CuCNLi_2$ in tetrahydrofuran prepared above. The reaction continued stirring for 1 h in the process of warming to –20 ^{o}C. The reaction mixture was poured into saturated sodium bicarbonate (10 mL) and extracted with EtOAc (4 X 10 mL). The combined extracts were dried over $MgSO_4$, filtered, and concentrated *in vacuo*. The residue was purified by flash column chromatography (30:1 hexanes/EtOAc + 1% Et_3N) to afford 0.068 g (65%) of vinyl stannane **2.44** as a light yellow oil. IR (neat) 2971, 2919, 1701, 1414, 1240 cm^{-1}; ^{1}H-NMR (500 MHz, $CDCl_3$) δ 4.18 (s broad, 2H), 3.76 (s, 3H), 3.44 (t, J = 6.0 Hz, 2H), 2.50 (m, 2H), 1.49 (s, 9H), 0.15 (s, 9H); ^{13}C-NMR (125 MHz, $CDCl_3$) δ 167.1, 162.1 broad, (154.6, 154.5), 133.2 broad, 79.7, 51.9, (44.4, 43.9), (40.5, 39.2), 33.1, 28.4, -7.6; HRMS (ESI) *m/z* 428.0868 [$(M+Na)^+$ calculated for $C_{15}H_{27}O_4NSnNa$: 428.0860].

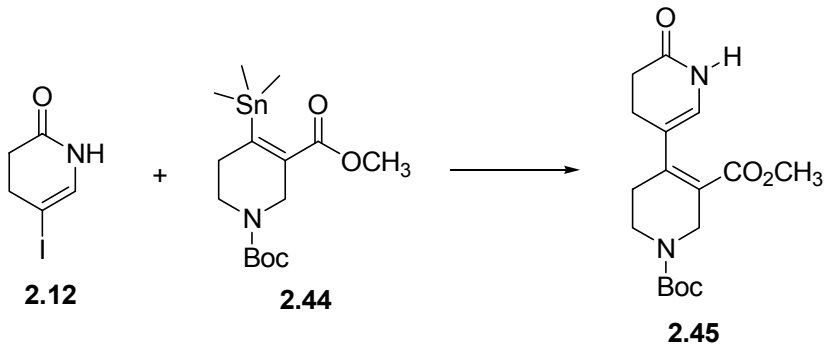

2.12 **2.44** **2.45**

Diene 2.45. To a solution of vinyl stannane **2.44** (0.051 g, 0.229 mmol) and beta-iodo enecarbamate **2.11** (0.084 g, 0.208 mmol) in DMSO (4 mL) was added $Pd(Ph_3P)_4$ (0.024 g, 0.0208 mmol) followed by CuCl (0.103 g, 1.042 mmol) and LiCl (0.053 g, 1.25

mmol) and the reaction mixture was vigorously degassed (3X) by the freeze-pump-thaw cycles (-78 $\rightarrow$ 25 ^{o}C, Ar). The reaction mixture was heated at 80 ^{o}C for 4.5 h. The reaction mixture was cooled, diluted with EtOAc (5 mL), and washed with a saturated sodium bicarbonate solution (10 mL). The aqueous layers were extracted with EtOAc (3 X 10 mL) and the combined organic layers were dried over $MgSO_4$, filtered, and concentrated *in vacuo*. The residue was purified by flash column chromatography (1:1:0.5 hexanes/EtOAc/MeOH) to afford 0.048 g (69%) of diene **2.45** as a light yellow oil. IR (neat) 3428 broad, 2972, 2928, 2359, 2336, 1692, 1420 cm^{-1}; ^{1}H-NMR (500 MHz, $CDCl_3$) δ 7.18 (d, J = 3.5 Hz, 1H), 5.97 (d, J = 4.5 Hz, 1H), 4.14 (s broad, 2H), 3.72 (s, 3H), 3.50 (t, J = 5.5 Hz, 2H), 2.57 (t, J = 7.5 Hz, 2H), 2.43 (t, J = 8.0 Hz, 2H), 2.30 (m, 2H); ^{13}C-NMR (125 MHz, $CDCl_3$) δ 170.8, 154.5 broad, 144.0, (132.1, 132.0), (128.6, 128.5), 121.7, 118.9, 80.1, 51.8, 43.9, 39.2, 30.4, 29.7, 28.4, 24.1; HRMS (ESI) *m/z* 343.1827 [$(M+Li)^+$ calculated for $C_{17}H_{24}N_2O_5Li$: 343.1845].

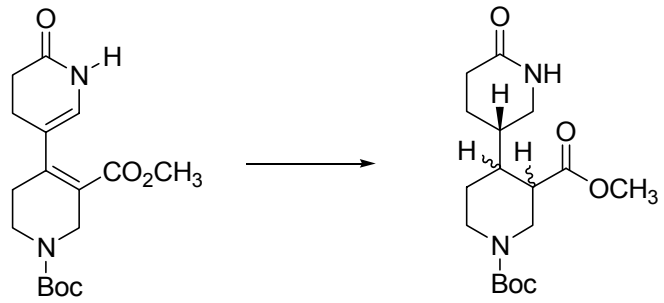

2.45 **2.46**

Hydrogenation Product 2.46. To a solution of diene **2.45** (0.033 g, 0.0985 mmol) in ethanol (4 mL) was added palladium (5% on activated carbon, 0.021 g, 0.00985 mmol). The reaction mixture was placed into a Parr Shaker and shaked under 40 psi of hydrogen at room temperature for 36 hours. The reaction mixture was filtered through a short pad of celite and washed with EtOAc (30 mL). The filtrate was concentrated *in vacuo*. The residue was purified by flash column chromatography (1:1:0.1 hexanes/EtOAc/MeOH) to afford 0.029 g (87%) of hydrogenation product **2.46** as a light yellow oil. IR (neat) 3421 broad, 1644, 1429, 1173 cm^{-1}; ^{1}H-NMR (500 MHz, DMSO, 75 ^{o}C) δ 7.11 (s broad, 1H), 4.22 (dd, J = 13.5, 7.5 Hz, 1H), 4.03 (m, 2H), 3.59 (s, 3H), 3.24-3.11 (m, 1H), 2.95 (t, J = 11.0 Hz, 1H), 2.89-2.83 (m, 1H), 2.75-2.62 (m, 2H), 2.20-2.14 (m, 1H), 2.12-2.01 (m, 1H), 1.91-1.87 (m, 1H), 1.81-1.73 (m, 2H), 1.66-1.64 (m, 1H), 1.58-1.52 (m, 1H), 1.44-1.37 (m, 1H), 1.37 (s, 9H); ^{13}C-NMR (125 MHz, DMSO, 75 ^{o}C) δ 173.1, (170.83, 170.78), 154.3, 79.2, (52.0, 51.8), (46.0, 45.9), (41.7, 41.6), 41.1, 35.8, (31.0, 30.9), 29.7, 28.8, 27.9, 25.2, 25.0; HRMS (ESI) *m/z* 341.2 [$(M+H)^{+}$ calculated for $C_{17}H_{29}N_2O_5$: 341.3].

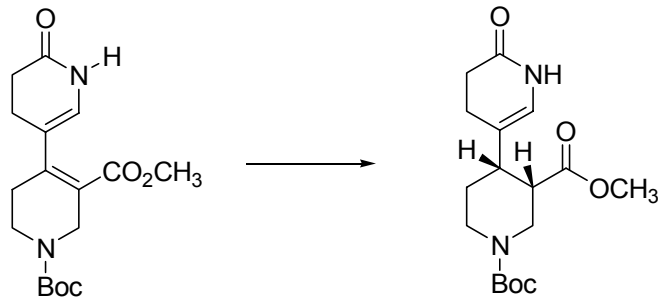

2.45 **2.47**

Partially Reduced Product 2.47. To a solution of diene **2.45** (0.078 g, 0.233 mmol) in ethanol (8 mL) was added palladium (5% on activated carbon, 0.049 g, 0.0233 mmol). The reaction mixture was placed into a Parr Shaker and shaked under 40 psi of hydrogen at room temperature for 24 hours. The reaction mixture was filtered through a short pad of celite and washed with EtOAc (40 mL). The filtrate was concentrated *in vacuo*. The residue was purified by flash column chromatography (1:1:0.1 hexanes/EtOAc/MeOH) to afford 0.017 g (22%) of partially reduced product **2.47** as a light yellow oil contaminated with hexanes as impurity. IR (neat) 3263 broad, 2930, 2356, 1737, 1685, 1434 cm^{-1}; ^{1}H-NMR (500 MHz, $CDCl_3$) δ 7.25 (s broad, 1H), 5.84 (d, J = 4.0 Hz, 1H), 4.44-4.16 (m, 2H), 3.62 (s, 3H), 3.07-2.97 (m, 1H), 2.82-2.77 (m, 2H), 2.48-2.44 (m, 2H), 2.42-2.40 (m, 1H), 2.40-2.33 (m, 2H), 2.26-2.14 (m, 2H), 1.45 (s, 9H); ^{13}C-NMR (125 MHz, $CDCl_3$) δ 172.1, 170.8, 154.6, 120.4, 118.7, 79.6, 51.4, (45.8, 44.9), (43.0, 42.4), 41.2, 30.3, 29.7, 28.3, 24.4, 23.5; HRMS (ESI) *m/z* 361.1716 [$(M+Na)^+$ calculated for $C_{17}H_{26}N_2O_5Na$: 361.1739].

CHAPTER III

SUMMARY

Chapter I provided background information concerning the biological activities of marine secondary metabolites. We also detailed some hypotheses which have been proposed by several groups to account for the biogenetic origin of these structurally novel marine macrocyclic diamine alkaloids.

Chapter II detailed our work towards the total synthesis of haliclonacyclamine C. Highlighting our synthesis is the successful use of a palladium-mediated coupling of a vinyl stannane and a vinyl iodide to construct the 3,4'linked bis-piperidine core structure. Our efforts to perform stereoselective hydrogenation of the coupled product were also discussed. In addition, we described the use of a VT-NMR experiment to analyze the hydrogenation product and the use of molecular modeling to predict the conformation of some important synthetic intermediates in the total synthesis of haliclonacyclamine C.

REFERENCES

1. Wayne Best's biological chemistry course's notes. Accessed: June 2004 http://home.it.net.au/~wmbest/biolchem/lecture-05.pdf

2. Faulkner, D. J. *Natural Product Reports* **2001**, *18*, 1.

3. Faulkner, D. J. *Natural Product Reports* **2002**, *19*, 1.

4. Bewley, C. A., Faulkner, D. J. *Angew. Chem. Int. Ed.* **1998**, *37*, 2163.

5. Sakai, R.; Higa, T. *J. Am. Chem. Soc.* **1986**, *108*, 6404.

6. Nakamura, H.; Deng, S.; Kobayashi, J.; Ohizumi, Y.; Tomotake, Y.; Matsuzaki, T. *Tetrahedron Lett.* **1987**, *6*, 621.

7. Baldwin, J. E.; Whitehead, R. C. *Tetrahedron Lett.* **1992**, *33*, 2059.

8. Sakai, R.; Kohmoto, S.; Higa, T.; Jefford, C. W.; Bernardinelli, G. *Tetrahedron Lett*. **1987**, *28*, 5493.

9. Garson, M. J. *Natural Product Reports* **1989**, *6*, 143

10. Cimino, G.; Destefano, S.; Scognamiglio, G.; Sodano, G.; Trivellone, E. *Bull. Soc. Chim. Belg.* **1986**, *95*, 783.

11. Kobayashi, J.; Tsuda, M.; Kawasaki, N.; Matsumoto, K.; Adachi, T. *Tetrahedron Lett.* **1994**, *35*, 4383.

12. Kong, F.; Anderson, R. J. *Tetrahedron* **1995**, *51*, 2895.

13. Baldwin, J. E.; Bischoff, L.; Claridge, T. D. W.; Heupel, F. A.; Spring, D. R.; Whitehead, R. C. *Tetrahedron* **1997**, *53*, 2271.

14. Baldwin, J. E.; Claridge, T. D. W.; Culshaw, A. J.; Heupel, F. A.; Lee, V.; Spring, D. R.; Whitehead, R. C.; Boughtflower, R. J.; Mutton, I. M.; Upton R. J. *Angew. Chem. Int. Ed.* **1998**, *37*, 2661.

15. Kaiser, A.; Billot, X.; Gateau-Olesker, A.; Marazano, C.; Das B. C. *J. Am. Chem. Soc.* **1998**, *120*, 8026.

16. Jakubowicz, K.; Abdeljelil, K. B.; Herdemann, M.; Martin, M.; Gateau-Olesker, A.; Mourabit, A. A.; Marazano, C.; Das B. C. *J. Org. Chem.* **1999**, *64*, 7381.

17. Becher, I. *Synthesis* **1980**, 589.

18. Cutignano, A.; Tramice, A.; De Caro, S.; Villani, G.; Cimino, G.; Fontana, A. *Angew. Chem. Int. Ed.* **2003**, *42*, 2633.

19. Cutignano, A.; Cimino, G.; Giordano, A.; Ippolito, G.; Fontana, A. *Tetrahedron Lett.* **2004**, *45*, 2627.

20. Clark, R. J.; Field, K. L.; Charan, R. D.; Garson, M. J.; Brereton I. M.; Willis, A. C. *Tetrahedron* **1998**, *54*, 8811.

21. Charan, R. D.; Garson, M. J.; Brereton I. M.; Willis, A. C.; Hooper, J. N. *Tetrahedron* **1996**, *52*, 9111.

22. Heck, R. F. *J. Am. Chem. Soc.* **1968**, *90*, 5518.

23. Nicolaou, K. C.; Sorensen, E. J. *Classics in Total Synthesis* VCH Publishers: New York, **1996**.

24. Beletskaya, I. P.; Cheprakov, A. V. *Chem. Rev.* **2000**, *100*, 3009.

25. Dieter, R. K.; Sharma, R. R. *J. Org. Chem.* **1996**, *61*, 4180.

26. Oliveira, D. F.; Miranda, P.; Correia, C. R. *J. Org. Chem.* **1999**, *64*, 6646.

27. Yu, C. Z.; Hu, L. Q. *Tetrahedron Lett.* **2001**, *42*, 5167.

28. Shono, T. *Tetrahedron* **1984**, *40*, 811.

29. Furstner, A.; Rumbo, A. *J. Org. Chem*. **2000**, *65*, 2608.

30. Jeffery, T. *Tetrahedron* **1996**, *52*, 10113.

31. Comins, D. L.; Dehghani, A. *Tetrahedron Lett.* **1992**, *33*, 6299.

32. Wulff, W. D.; Peterson, G. A.; Bauta, W. E.; Chan, K.-S.; Faron, K. L.; Gilbertson, S. R.; Kaesler, R. W.; Yang, D. C.; Murray, C. K. *J. Org. Chem.* **1986**, *51*, 277.

33. Sharma, S.; Oehlschlager, A. C. *J. Org. Chem*. **1991**, *56*, 770.

34. Han, X.; Stoltz, B. M.; Corey, E. J. *J. Am. Chem. Soc.* **1999**, *121*, 7600.

35. Ojima, I.; Korda, A.; Shay, W. R. *J. Org. Chem*. **1991**, *56*, 2024.

36. Chandrasekhar, S.; Babu, B. N.; Reddy, C. R. *Tetrahedron Lett.* **2003**, *44*, 2057.

37. Christoffers, J.; Scharl, H. *Eur. J. Org. Chem.* **2002**, *9*, 1505.

38. Comins, D. L.; Dehghani, A.; Foti, C. J.; Joseph, S. P. *Organic Syntheses*, **CV9**, 1505.

APPENDIX

SELECTED SPECTRA RELEVANT TO CHAPTER II

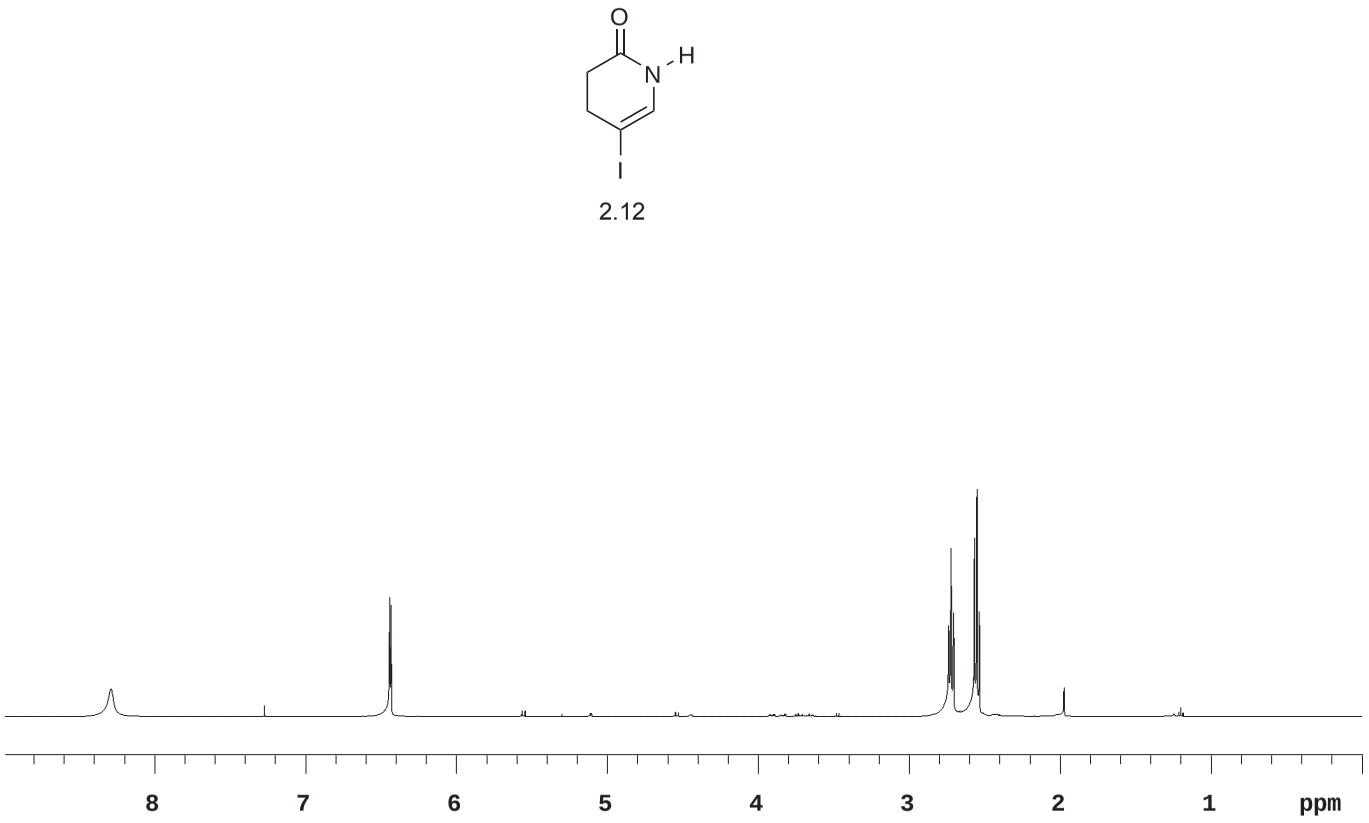

2.12

Figure 12 The 500 MHz ^{1}H NMR spectrum of **2.12** in $CDCl_3$

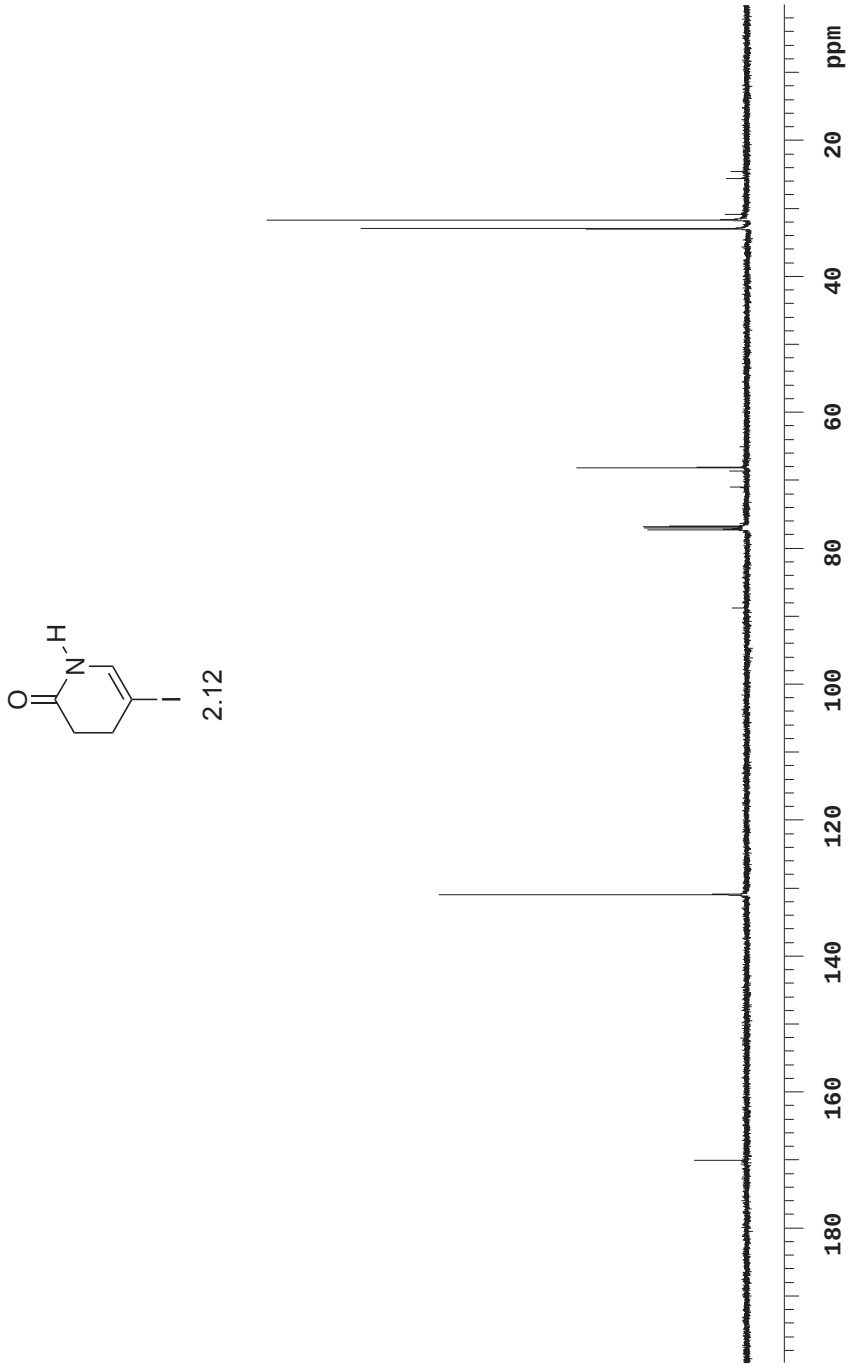

Figure 13 The 125 MHz ^{13}C NMR spectrum of **2.12** in $CDCl_3$

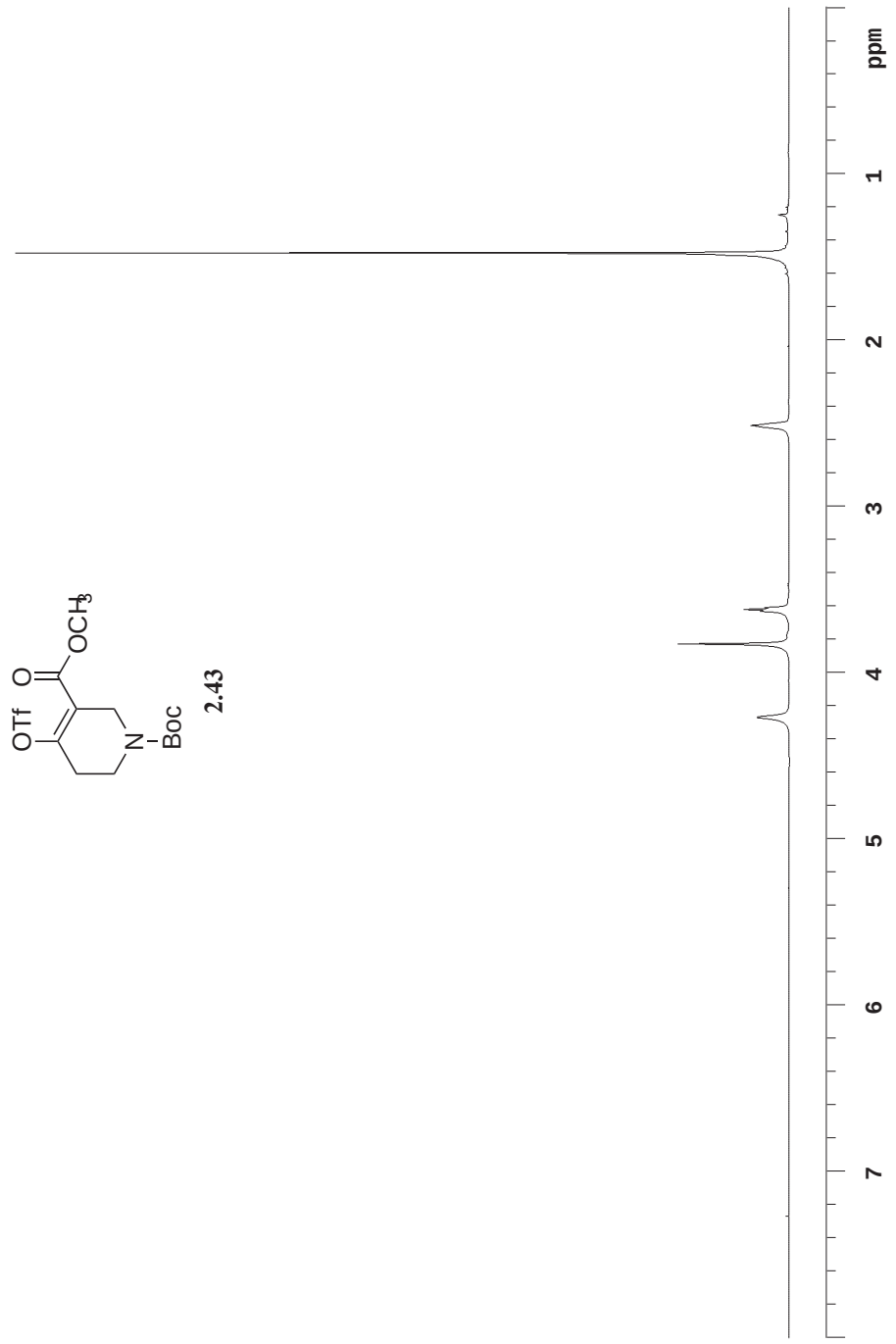

Figure 14 The 500 MHz ^{1}H NMR spectrum of **2.43** in $CDCl_3$

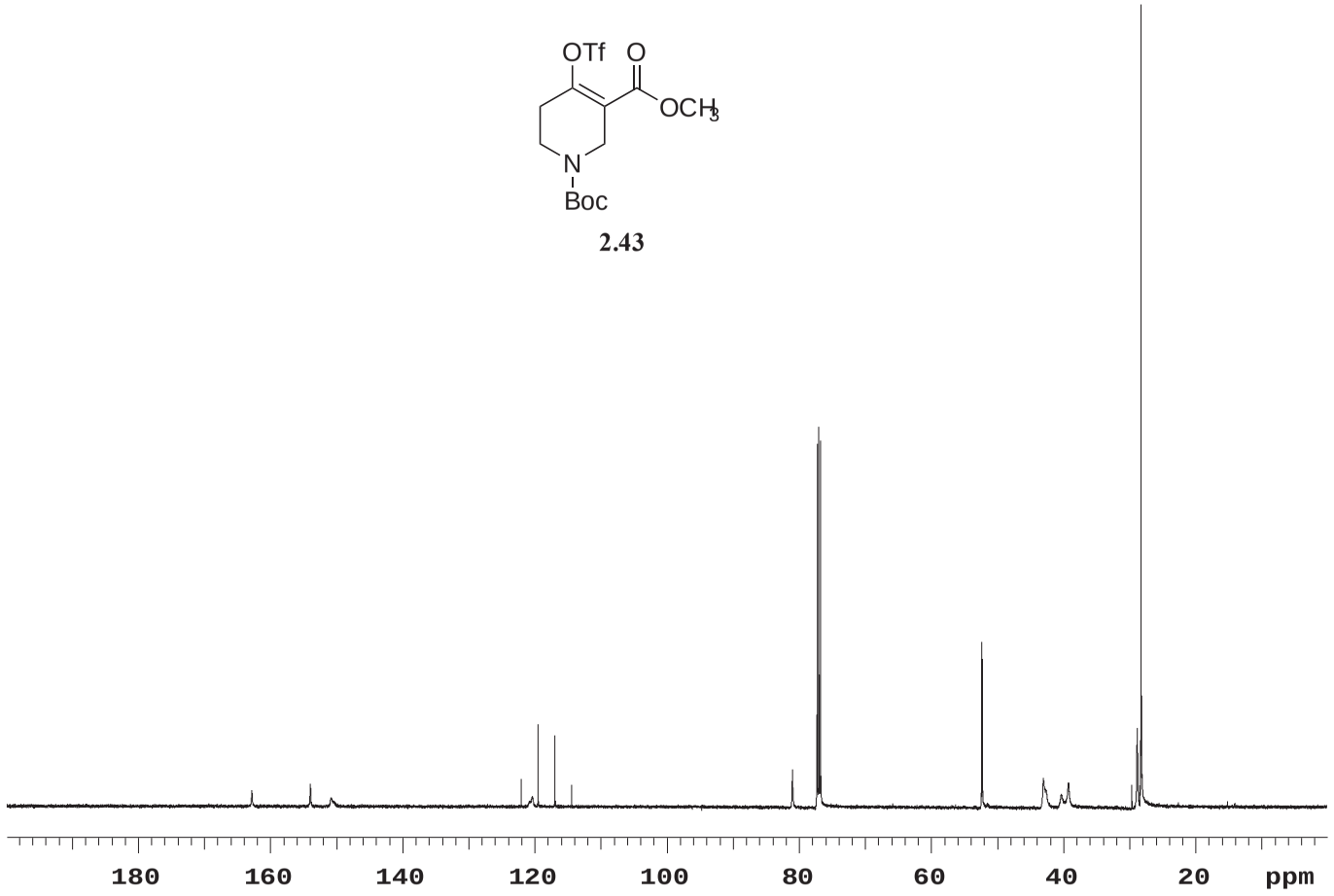

Figure 15 The 125 MHz ^{13}C NMR spectrum of **2.43** in $CDCl_3$

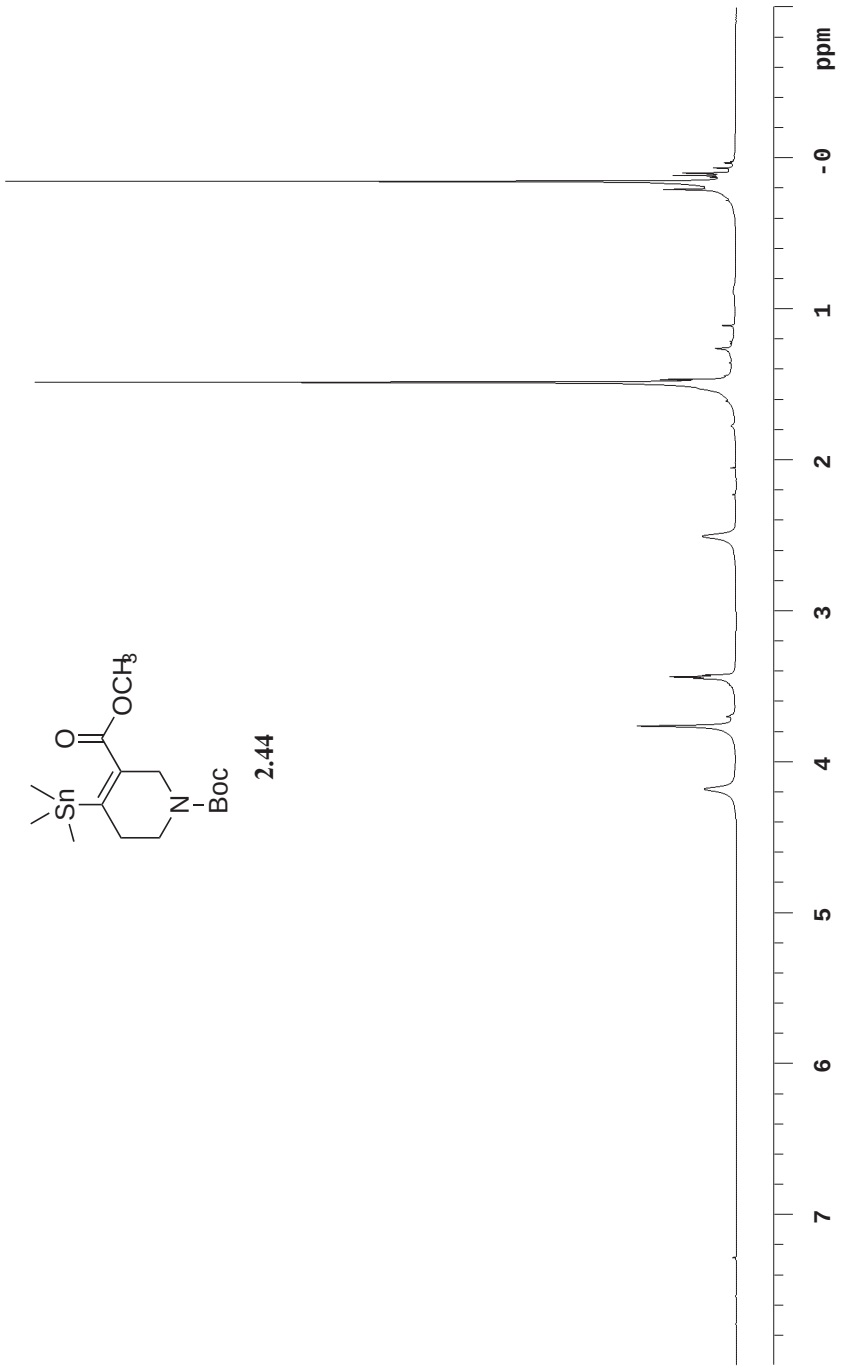

Figure 16 The 500 MHz ^{1}H NMR spectrum of **2.44** in $CDCl_3$

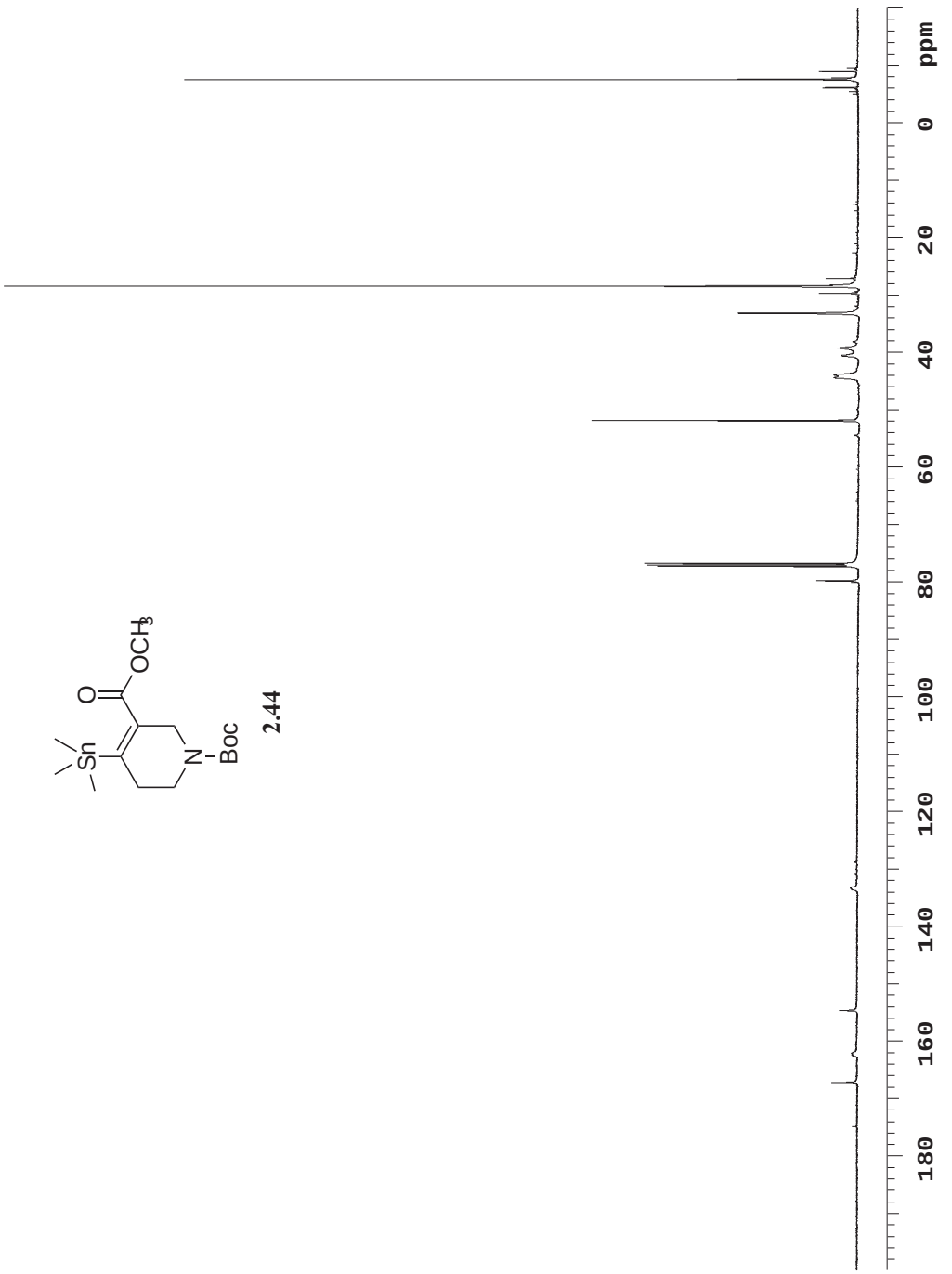

Figure 17 The 125 MHz ^{13}C NMR spectrum of **2.44** in $CDCl_3$

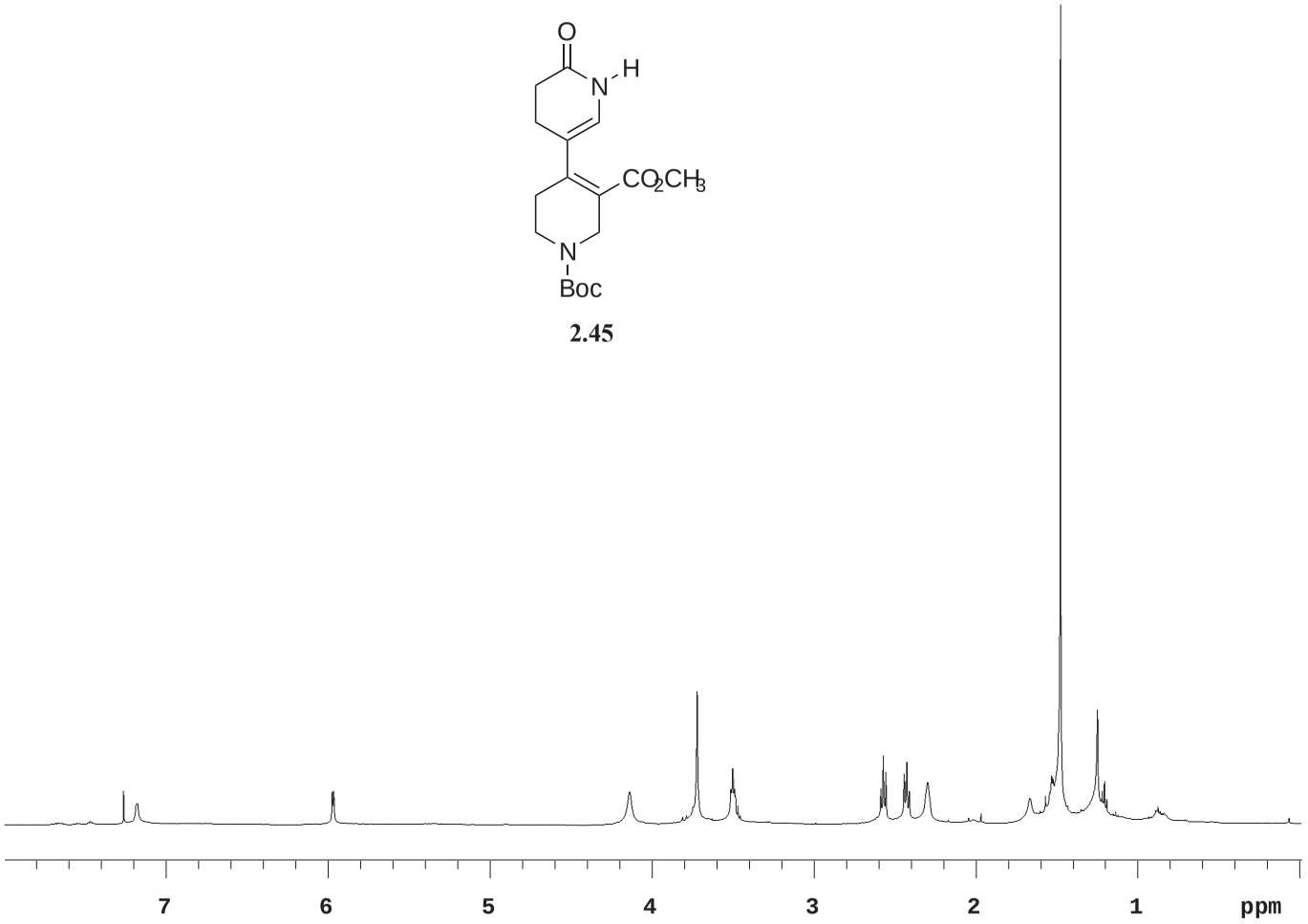

Figure 18 The 500 MHz ^{1}H NMR spectrum of **2.45** in $CDCl_3$

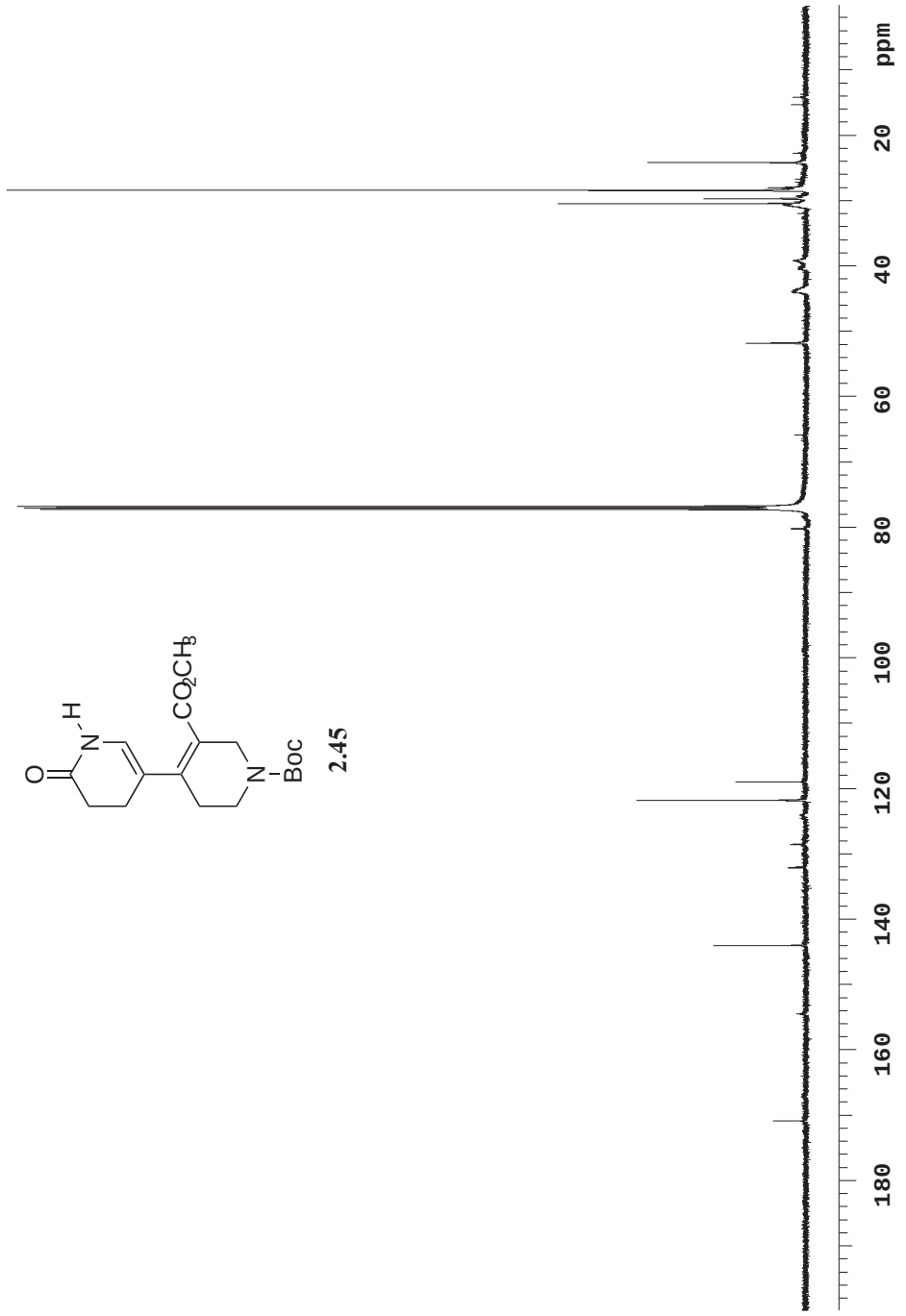

Figure 19 The 125 MHz ^{13}C NMR spectrum of **2.45** in $CDCl_3$

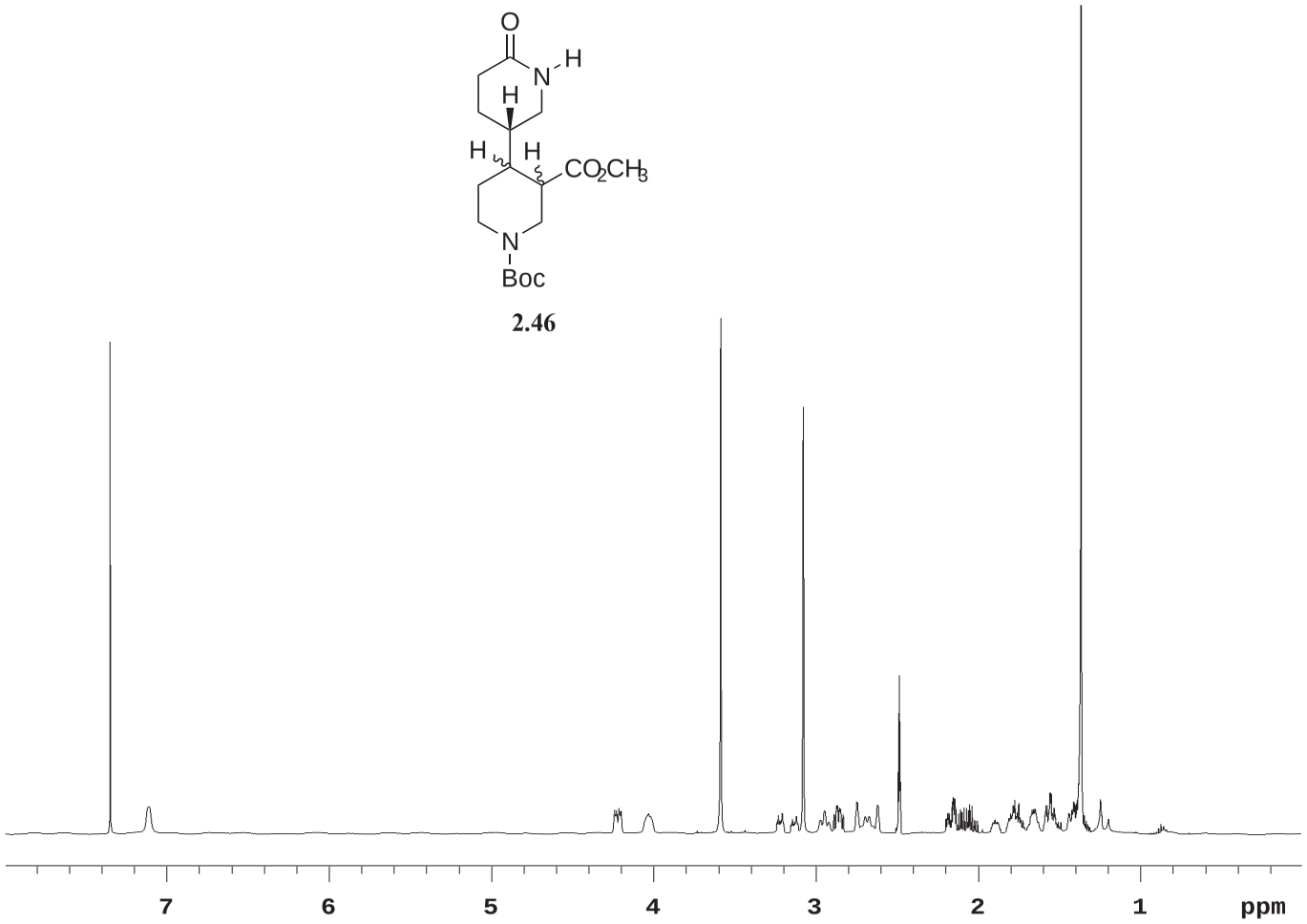

Figure 20 The 500 MHz ^{1}H NMR (75 ^{o}C) spectrum of **2.46** in $(CD_3)_2SO$

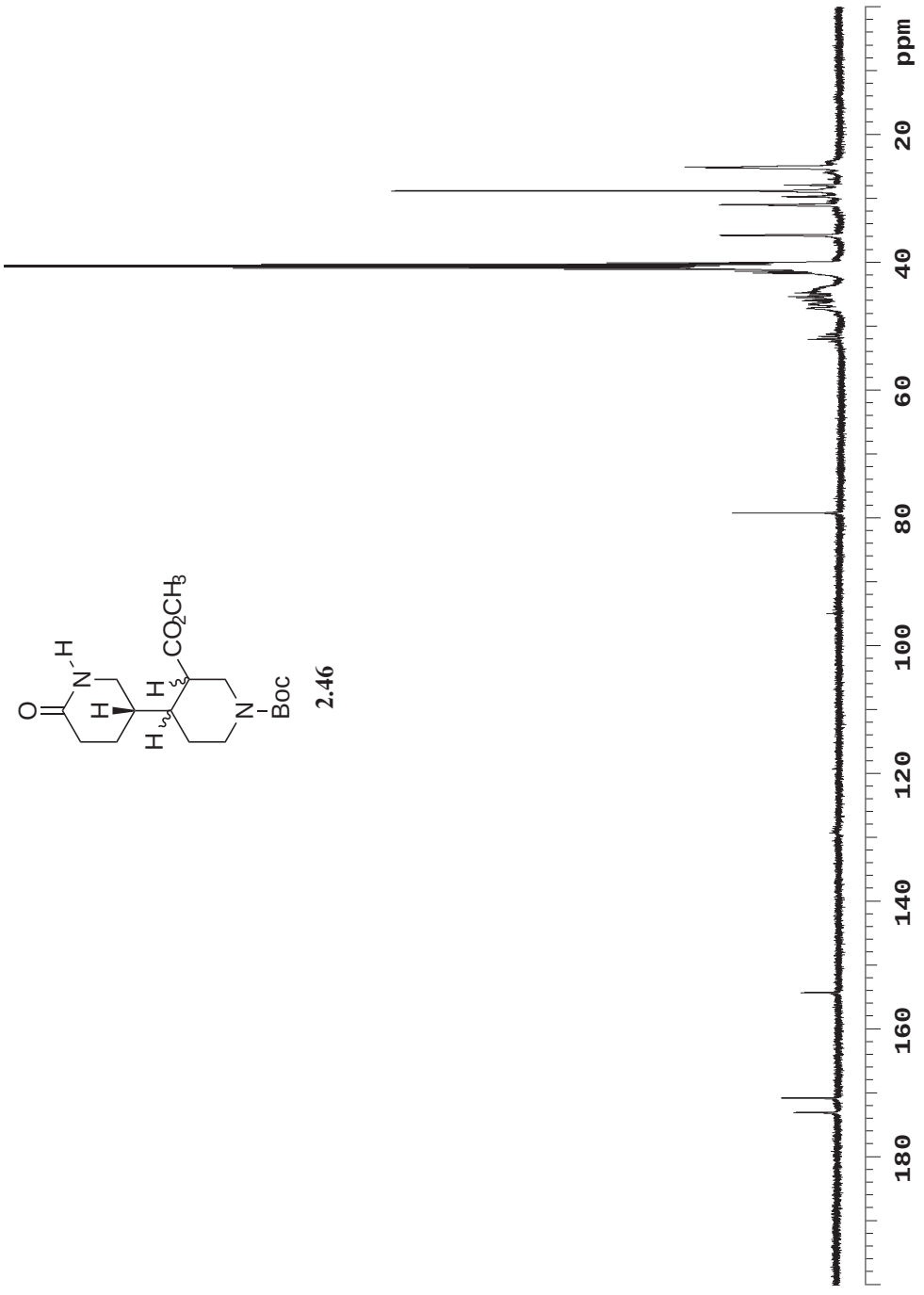

Figure 21 The 125 MHz ^{13}C NMR (75 ^{o}C) spectrum of **2.46** in $(CD_3)_2SO$

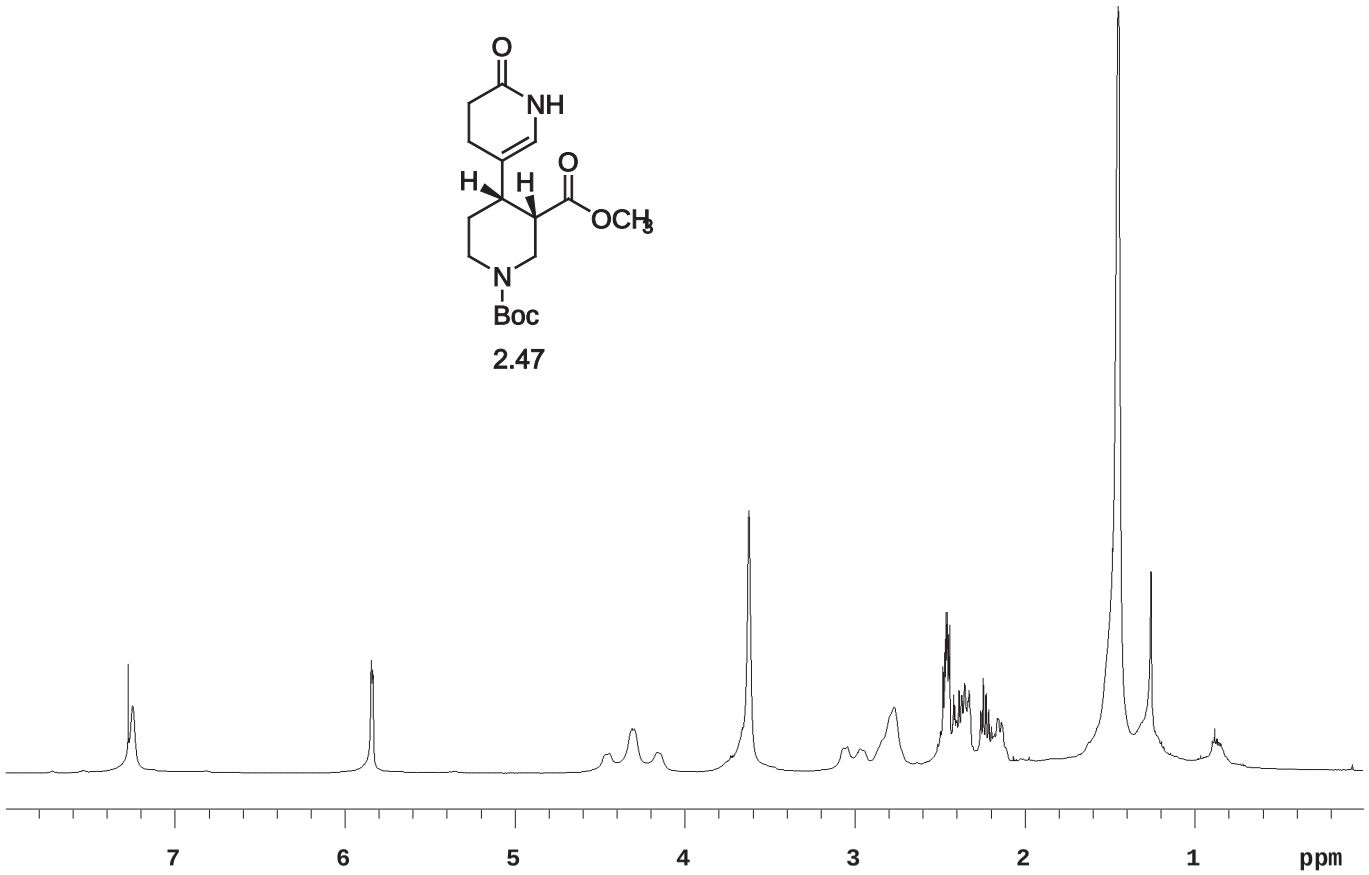

Figure 22 The 500 MHz ^{1}H NMR spectrum of **2.47** in $CDCl_3$

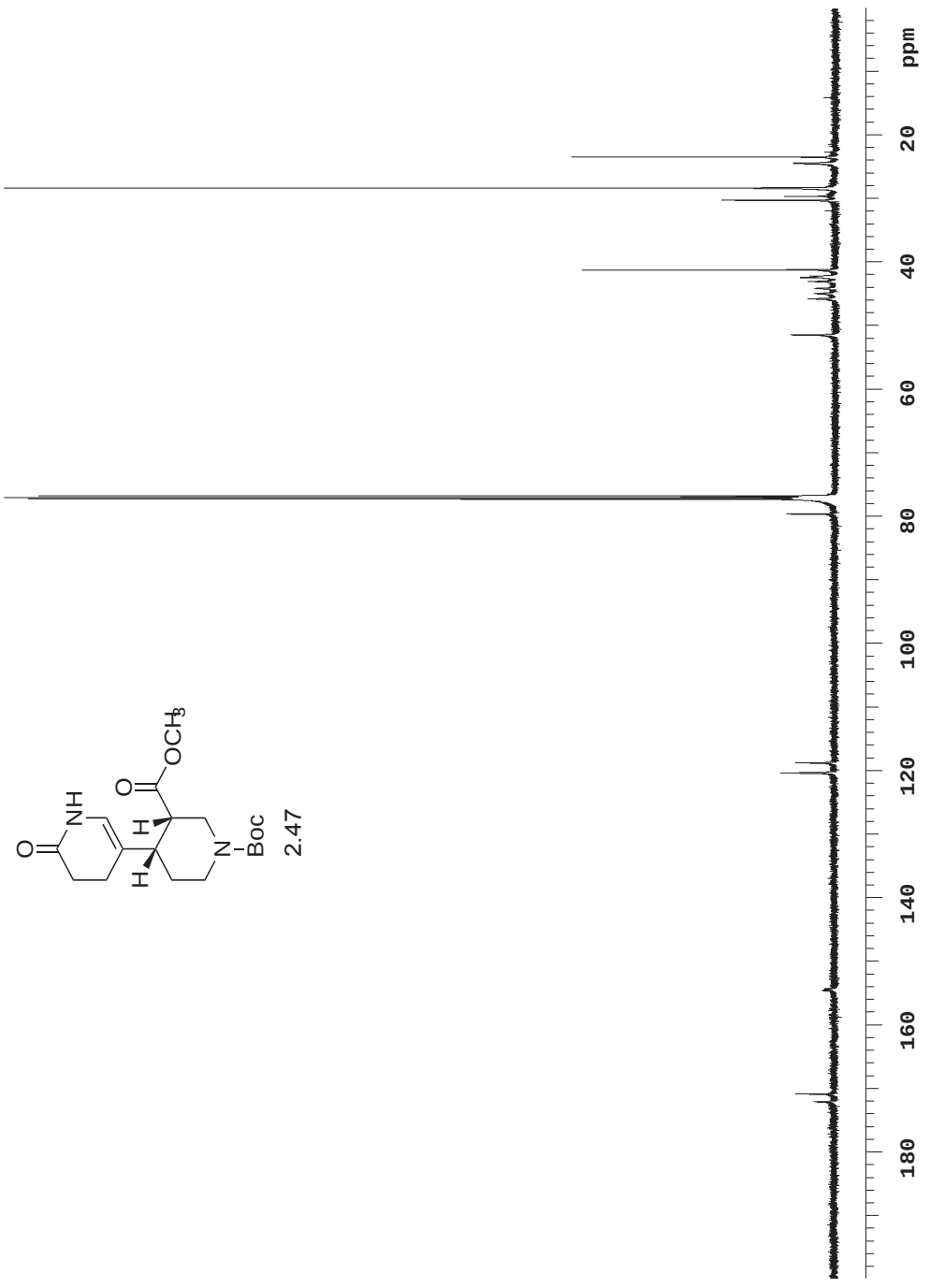

Figure 23 The 125 MHz ^{13}C NMR spectrum of **2.47** in $CDCl_3$

VITA

TAO QU

Permanent Address:

Room 402
No. 20-3, Mujie Street
Harbin, 150001
P. R. China

Educational Background:

B.S., Chemistry, Peking University, China, 2001.
M.S., Chemistry, Texas A&M University, 2004.

Publications:

"Synthesis of pseudo-Apoptolidin and Structural Corroboration of Apoptolidin." Wu, B.; Jin, B.; Qu, T.; Liu, Q.; Sulikowski, G. A. *Abstracts of Papers of the Am. Chem. Soc.* **2003**, *225*, 247-ORGN.

"Studies on the Synthesis of Apoptolidin: Stereocontrolled Assembly of the C(7)-C(28) Fragment." Wu, B.; Liu, Q.; Qu, T.; Sulikowski, G. A. *Org. Lett.* submitted.